Improved general solution for the dynamic modeling of Gough–Stewart platform based on principle of virtual work

Hadi Kalani, Amir Rezaei & Alireza Akbarzadeh

Nonlinear Dynamics
An International Journal of Nonlinear Dynamics and Chaos in Engineering Systems

ISSN 0924-090X
Volume 83
Number 4

Nonlinear Dyn (2016) 83:2393-2418
DOI 10.1007/s11071-015-2489-z

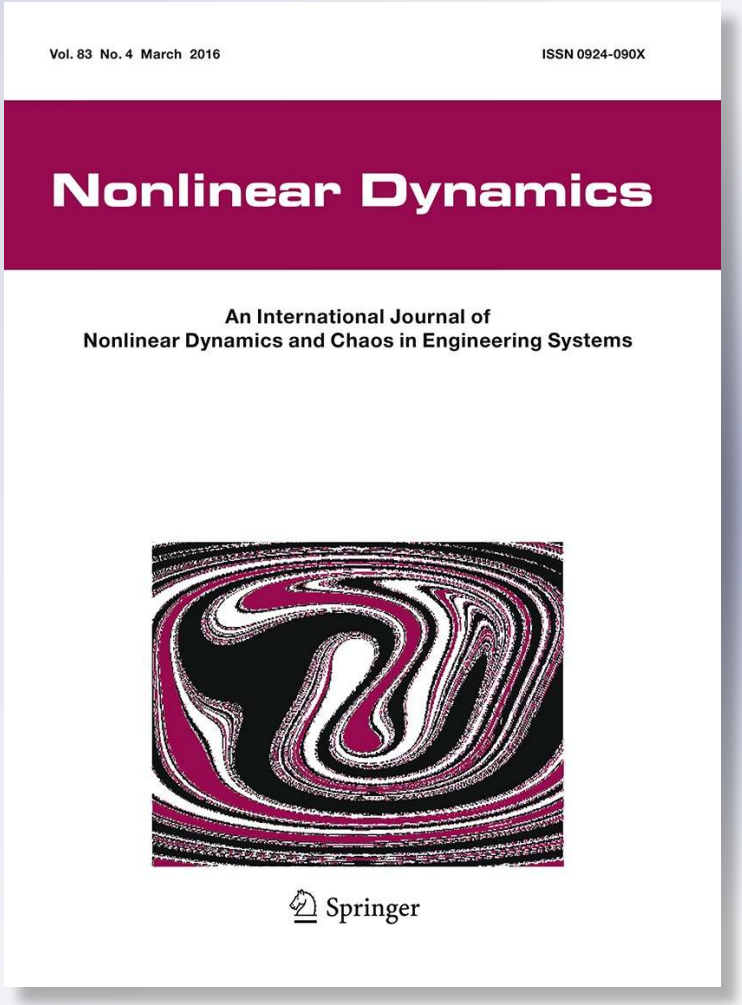

Springer

Nonlinear Dyn (2016) 83:2393–2418
DOI 10.1007/s11071-015-2489-z

ORIGINAL PAPER

Improved general solution for the dynamic modeling of Gough–Stewart platform based on principle of virtual work

Hadi Kalani · Amir Rezaei · Alireza Akbarzadeh

Received: 22 August 2014 / Accepted: 3 November 2015 / Published online: 26 November 2015

Abstract This paper presents an improved general dynamic formulation, inverse and direct dynamics, of 6-UPS Gough–Stewart parallel robot based on the virtual work method. The new formulation offers a reduction in the computational time and improves accuracy of the dynamics equations. This method allows elimination of constraint forces/moments at the passive joints from equations of motion. Since, the dynamic formulations are derived in joint space, the concept of direct link Jacobian matrices are employed to obtain all rigid bodies' twists. The direct link Jacobian matrices convert the twist of the rigid bodies to actuated joints velocities. Moreover, more accurate formulation is obtained by considering the angular velocity and acceleration vectors of the robot's legs. In the process of solving the direct dynamics problem, a modified hybrid strategy is employed to obtain the near-exact solution for the direct kinematics problem (DKP). The modified hybrid strategy combines the artificial neural network and the third-order Newton–Raphson method. This strategy satisfies both goals to find the nearest exact solution and reduces execution time for the DKP. Next, two numerical examples are presented and the results are verified using a commercial dynamics modeling software. Finally, for comparison, Euler–Lagrange formulation is also obtained. Results indicates that the proposed dynamics formulation offers a significant improvement in both accuracy and execution time.

Keywords Direct dynamic analysis · Principle of virtual work · Modified hybrid strategy · Link Jacobian matrix

H. Kalani · A. Rezaei · A. Akbarzadeh (✉)
Mechanical Engineering Department, Center of Excellence on Soft Computing and Intelligent Information Processing (SCIIP), Ferdowsi University of Mashhad, Mashhad, Iran
e-mail: ali_akbarzadeh@um.ac.ir

H. Kalani
e-mail: hadi.kalani@yahoo.com

A. Rezaei
e-mail: amirrezaei_aico@stu.um.ac.ir

List of symbols

$\mathrm{B}\{x, y, z\}$	Fixed coordinate frame which is attached to center of fixed platform
$\mathrm{T}\{u, v, w\}$	Moving coordinate frame which is attached to center of moving platform, P
$\{\mathcal{F}i\}$	Local coordinate frames which is attached to ith cylinder at ith passive U-joint
α_i	A constant value denotes the angle of vector of ${}^{\mathrm{B}}\mathbf{a}_i$, about x-axis of frame {B}
γ_i	Rotation angle of ith passive U-joint about y-axis of local frame $\{\mathrm{B}_i\}$
ψ_i	Rotation angle of ith passive U-joint about x-axis of local frame $\{\mathrm{T}_i\}$
${}^{\mathrm{B}}_{\mathrm{T}}\mathbf{R}$	Rotation matrix to transfer a vector defined in {T} to {B}

${}^{\mathrm{B}}_{\mathcal{F}i}\mathbf{R}$	Rotation matrix to transfer a vector defined in $\{\mathcal{F}i\}$ to $\{\mathrm{B}\}$ for ith U-joint
${}^{\tau}\boldsymbol{\vartheta}$	Arbitrary $\boldsymbol{\vartheta}$ vector that is defined in arbitrary coordinate frame $\{\tau\}$
$a_1, \ldots, a_6$	Distance between the center of fixed platform and passive U-joints
$b_1, \ldots, b_6$	Distance between the center of moving platform and passive S-joints
$q_1^{\mathrm{ac}}, \ldots, q_6^{\mathrm{ac}}$	Translational variables for the actuated prismatic joint
$x_{\mathrm{P}}, y_{\mathrm{P}}, z_{\mathrm{P}}$	Translational variables of the tool tip, point P
θ, φ, λ	The Euler angles about the x-, y- and z-axes of moving platform
e_1	Center of gravity for cylindrical part of the actuated prismatic joints
e_2	Center of gravity for position of the actuated prismatic joints
$\mathbf{a}_i$	Position vector located on ith passive U-joint in frame $\{\mathrm{B}\}$
$\mathbf{b}_i$	Position vector connecting the end-effector to the ith passive S-joint, S_i
$\mathbf{q}_i^{\mathrm{ac}}$	Position vector which specifies length of ith actuated prismatic joint
$\mathbf{p}$	Position vector of the tool tip, point P
$\hat{\mathbf{q}}_i^{\mathrm{ac}}$	Unit vector along ith actuated link
$\mathbf{r}_{1i}, \mathbf{r}_{2i}$	Position vectors located on the center of gravity of ith actuator's cylinder and piston
$\dot{\mathrm{q}}_1^{\mathrm{ac}}, \ldots, \dot{\mathrm{q}}_6^{\mathrm{ac}}$	Values of prismatic actuated joints rate
$\dot{\mathrm{x}}_{\mathrm{P}}, \dot{\mathrm{y}}_{\mathrm{P}}, \dot{\mathrm{z}}_{\mathrm{P}}$	Values of Cartesian velocities of the tool tip
$\omega_x, \omega_y, \omega_z$	Values of angular velocities of the moving platform
$\dot{\mathrm{x}}_{\mathrm{S}i}, \dot{\mathrm{y}}_{\mathrm{S}i}, \dot{\mathrm{z}}_{\mathrm{S}i}$	Values for velocities of the ith passive S-joint, S_i
$\ddot{\mathrm{q}}_1^{\mathrm{ac}}, \ldots, \ddot{\mathrm{q}}_6^{\mathrm{ac}}$	Values of prismatic actuated joints acceleration
$\ddot{\mathrm{x}}_{\mathrm{P}}, \ddot{\mathrm{y}}_{\mathrm{P}}, \ddot{\mathrm{z}}_{\mathrm{P}}$	Values of Cartesian accelerations of the tool tip
$\dot{\omega}_x, \dot{\omega}_y, \dot{\omega}_z$	Values of angular accelerations of the moving platform
$\ddot{\mathrm{x}}_{\mathrm{S}i}, \ddot{\mathrm{y}}_{\mathrm{S}i}, \ddot{\mathrm{z}}_{\mathrm{S}i}$	Values for accelerations of the ith passive S-joint, S_i
$\dot{\mathbf{q}}^{\mathrm{ac}}$	Vector of the prismatic actuated joint rates, $\{\dot{\mathrm{q}}_1^{\mathrm{ac}} \quad \ldots \quad \dot{\mathrm{q}}_6^{\mathrm{ac}}\}^{\mathrm{T}}$
$\boldsymbol{v}_{\mathrm{P}}$	Cartesian velocity vector for the tip, $\{v_{\mathrm{P}x} \quad v_{\mathrm{P}y} \quad v_{\mathrm{P}z}\}^{\mathrm{T}} = \{\dot{\mathrm{x}}_{\mathrm{P}}, \quad \dot{\mathrm{y}}_{\mathrm{P}}, \quad \dot{\mathrm{z}}_{\mathrm{P}}\}^{\mathrm{T}}$
$\boldsymbol{\omega}_{\mathrm{MP}}$	Angular velocity vector of the moving platform, $\{\omega_x \quad \omega_y \quad \omega_z\}^{\mathrm{T}}$
$\boldsymbol{v}_{\mathrm{S}i}$	Velocity vector of the ith spherical joint, $\{\dot{\mathrm{x}}_{\mathrm{S}_i}, \quad \dot{\mathrm{y}}_{\mathrm{S}_i}, \quad \dot{\mathrm{z}}_{\mathrm{S}_i}\}^{\mathrm{T}}$
$\boldsymbol{\omega}_{\mathrm{Leg},i}$	Angular velocity of the ith actuated link
$\boldsymbol{v}_{\mathrm{C.G.1}\,i}$	Cartesian velocity of the mass center of ith actuator's cylinder
$\boldsymbol{v}_{\mathrm{C.G.2}\,i}$	Cartesian velocity of the mass center of ith actuator's piston
$\ddot{\mathbf{q}}^{\mathrm{ac}}$	Vector of the prismatic actuated joint accelerations, $\{\ddot{\mathrm{q}}_1^{\mathrm{ac}}, \ldots, \ddot{\mathrm{q}}_6^{\mathrm{ac}}\}^{\mathrm{T}}$
$\dot{\boldsymbol{v}}_{\mathrm{P}}$	Cartesian acceleration vector for the tip, $\{\dot{v}_{\mathrm{P}x}\dot{v}_{\mathrm{P}y}\dot{v}_{\mathrm{P}z}\}^{\mathrm{T}} = \{\ddot{\mathrm{x}}_{\mathrm{P}}, \ddot{\mathrm{y}}_{\mathrm{P}}, \ddot{\mathrm{z}}_{\mathrm{P}}\}^{\mathrm{T}}$
$\dot{\boldsymbol{\omega}}_{\mathrm{MP}}$	Angular acceleration vector of the moving platform, $\{\dot{\omega}_x \quad \dot{\omega}_y \quad \dot{\omega}_z\}^{\mathrm{T}}$
$\dot{\boldsymbol{v}}_{\mathrm{S}i}$	Acceleration vector of the ith spherical joint, $\{\ddot{\mathrm{x}}_{\mathrm{S}_i}, \quad \ddot{\mathrm{y}}_{\mathrm{S}_i}, \quad \ddot{\mathrm{z}}_{\mathrm{S}_i}\}^{\mathrm{T}}$
$\dot{\boldsymbol{\omega}}_{\mathrm{Leg},i}$	Angular acceleration of the ith actuated link
$\dot{\boldsymbol{v}}_{\mathrm{C.G.1}\,i}$	Cartesian acceleration of the mass center of ith actuator's cylinder
$\dot{\boldsymbol{v}}_{\mathrm{C.G.2}\,i}$	Cartesian acceleration of the mass center of ith actuator's piston
$\dot{\mathbf{t}}_{\mathrm{MP}}$	Twist vector of the moving platform, $\{\boldsymbol{v}_{\mathrm{P}}^{\mathrm{T}} \quad \boldsymbol{\omega}_{\mathrm{MP}}^{\mathrm{T}}\}^{\mathrm{T}}$
${}^{\mathcal{F}i}\mathbf{t}_{\mathrm{cyl},i}$	Twist vector of ith actuator's cylinder
${}^{\mathcal{F}i}\mathbf{t}_{\mathrm{pis},i}$	Twist vector of ith actuator's piston
$\dot{\mathbf{t}}_{\mathrm{MP}}$	Vector of the moving platform acceleration, $\{\dot{\boldsymbol{v}}_{\mathrm{P}}^{\mathrm{T}} \quad \dot{\boldsymbol{\omega}}_{\mathrm{MP}}^{\mathrm{T}}\}^{\mathrm{T}}$
${}^{\mathcal{F}i}\dot{\mathbf{t}}_{\mathrm{cyl},i}$	Acceleration vector of ith actuator's cylinder, $\left\{{}^{\mathcal{F}i}\dot{\boldsymbol{v}}_{\mathrm{C.G.1}i}^{\mathrm{T}} \quad {}^{\mathcal{F}i}\dot{\boldsymbol{\omega}}_{\mathrm{Leg},i}^{\mathrm{T}}\right\}^{\mathrm{T}}$ in $\{\mathcal{F}i\}$
${}^{\mathcal{F}i}\dot{\mathbf{t}}_{\mathrm{psi},i}$	Acceleration vector of ith actuator's piston, $\{{}^{\mathcal{F}i}\dot{\boldsymbol{v}}_{\mathrm{C.G.2}i}^{\mathrm{T}} \quad {}^{\mathcal{F}i}\dot{\boldsymbol{\omega}}_{\mathrm{Leg},i}^{\mathrm{T}}\}^{\mathrm{T}}$ in $\{\mathcal{F}i\}$
$\mathbf{J}_{\mathrm{MP}i}$	A 3×6 matrix which maps $\mathbf{t}_{\mathrm{MP}}$ to velocity of the ith spherical joint, $\boldsymbol{v}_{\mathrm{S}i}$
$\mathbf{J}_{\mathrm{MP}}$	Inverse Jacobian matrix (6×6matrix) which maps $\mathbf{t}_{\mathrm{MP}}$ to $\dot{\mathbf{q}}^{\mathrm{ac}}$
$\mathbf{J}_{\omega i}$	A 3×6 matrix which maps $\mathbf{t}_{\mathrm{MP}}$ to ${}^{\mathcal{F}i}\boldsymbol{\omega}_{\mathrm{Leg},i}$
$\mathbf{J}_{v1,i}$	A 3×6 matrix which maps $\mathbf{t}_{\mathrm{MP}}$ to ${}^{\mathcal{F}i}\boldsymbol{v}_{\mathrm{C.G.1}i}$
$\mathbf{J}_{v2,i}$	A 3×6 matrix which maps $\mathbf{t}_{\mathrm{MP}}$ to ${}^{\mathcal{F}i}\boldsymbol{v}_{\mathrm{C.G.2}i}$
$\mathbf{J}_{\mathrm{inv,cyl},i}$	Inverse ith link Jacobian matrix (6×6matrix) which maps $\mathbf{t}_{\mathrm{MP}}$ to ${}^{\mathcal{F}i}\mathbf{t}_{\mathrm{cyl},i}$
$\mathbf{J}_{\mathrm{inv,pis},i}$	Inverse ith link Jacobian matrix (6×6matrix) which maps $\mathbf{t}_{\mathrm{MP}}$ to ${}^{\mathcal{F}i}\mathbf{t}_{\mathrm{pis},i}$

$\mathbf{J}_{\mathrm{dir,cyl},i}$	Direct ith link Jacobian matrix (6×6 matrix) which maps $\mathbf{t}_{\mathrm{MP}}$ to $\dot{\mathbf{q}}^{\mathrm{ac}}$
$\mathbf{J}_{\mathrm{dir,pis},i}$	Direct ith link Jacobian matrix (6×6 matrix) which maps $\mathbf{t}_{\mathrm{MP}}$ to $\dot{\mathbf{q}}^{\mathrm{ac}}$
$\mathbf{w}_{\mathrm{ext}}$	Applied external wrench exerted to end-effector define in {B}
$\mathbf{f}^{\mathrm{ac}}$	Actuated joints forces
$\mathbf{w}_{\mathrm{MP}}$	Resultant wrench due to external wrench and inertia of the moving platform
${}^{\mathcal{F}i}\mathbf{w}_{\mathrm{cyl},i}$	Resultant wrench due to inertia of ith actuator's cylinder defined in $\{\mathcal{F}i\}$
${}^{\mathcal{F}i}\mathbf{w}_{\mathrm{pis},i}$	Resultant wrench due to inertia of ith actuator's piston defined in $\{\mathcal{F}i\}$
$\delta\,\mathbf{q}^{\mathrm{ac}}$	Virtual translational vector of actuated joints
$\delta\,\mathbf{t}_{\mathrm{MP}}$	Virtual twist vector of the moving platform
$\delta^{\mathcal{F}i}\mathbf{t}_{\mathrm{cyl},i}$	Virtual twist vector of ith actuator's cylinder defined in $\{\mathcal{F}i\}$
$\delta^{\mathcal{F}i}\,\mathbf{t}_{\mathrm{pis},i}$	Virtual twist vector of ith actuator's piston defined in $\{\mathcal{F}i\}$
m_{MP}	Mass of the moving platform
$m_{\mathrm{cyl},i}$	Mass of the ith actuator's cylinder
$m_{\mathrm{pis},i}$	Mass of the ith actuator's piston
$\mathbf{g}$	Gravitational acceleration vector defined in {B} , $\mathbf{g} = \{0 \quad 0 \quad 9.81\}^{\mathrm{T}}$
${}^{\mathrm{B}}\mathbf{I}_{\mathrm{MP}}$	Inertia matrix of the moving platform with respect to the base frame, {B}
${}^{\mathcal{F}i}\mathbf{I}_{\mathrm{cyl},i}$	Inertia matrix of ith actuator's cylinder defined in $\{\mathcal{F}i\}$
${}^{\mathcal{F}i}\mathbf{I}_{\mathrm{pis},i}$	Inertia matrix of ith actuator's piston defined in $\{\mathcal{F}i\}$

1 Introduction

The Gough–Stewart platform is a type of parallel manipulator, which consists of a mobile platform and a stationary base, connected to each other using six linear actuators. The first structure of this robot with spherical joints at both end of a leg is called 6-SPS (*Spherical–Prismatic–Spherical*) Gough–Stewart platform, while the second one, having a universal joint at the base and a spherical joint at the moving platform is called 6-UPS (*Universal–Prismatic–Spherical*) Gough–Stewart platform. A number of studies exist on the kinematics, dynamics and control of parallel manipulators. Kinematics problems can be divided into two different branches: direct kinematics problems (DKP) and inverse kinematics problems (IKP). In inverse kinematics, we determine the leg lengths given the position and orientation of the mobile platform. In the direct kinematics, we determine position and orientation of the mobile platform by giving leg lengths. Unlike serial manipulators, the application of inverse dynamic for parallel manipulators in control requires the additional solution of the direct kinematics [1]. In the inverse dynamics, the desired trajectory of the end-effector as well as the mass distribution of each link is given, and the required actuator moments and/or forces necessary to generate this trajectory are determined. In the direct dynamics, initial actuated joint positions, initial actuated joint velocities, applied actuated torques, applied external forces to end-effector, and the mass distribution of all links are supplied, and the resulting motion of the end-effector is determined [2–4]. Several approaches have been employed to solve inverse dynamic of Gough–Stewart robot including the Newton–Euler laws [5–9], the Euler–Lagrange formulation [10–14] and the principle of the virtual work [15,16]. Although to the best of author's knowledge, only two studies, Kane's method [17] and the Newton–Euler method [18], exists for obtaining the direct dynamic of Gough–Stewart Platform. The Newton–Euler formulation is obtained from the free-body diagrams. The approach is not suitable for motion simulation, as it finds the internal moments and forces that do not affect the motion of the system [2–4,17]. The Euler–Lagrange equations results from the kinetic and potential energies of the system. Euler–Lagrange equations give an independent set of equations of motion that is good for motion simulation; however, it requires complex calculations of partial derivatives. The principle of virtual work is the most efficient method for the dynamic analysis of parallel manipulators. This method allows elimination of all reaction forces and moments. Moreover, one can derive the equations of motions in terms of independent generalized coordinates. The virtual work method is an efficient approach to derive dynamic equations for the inverse dynamics of the Gough–Stewart platform. However, for the direct dynamics, the method of virtual work is not straightforward because of the complicated velocity transform between the joint space and task space [17]. In this study, we present a novel method to overcome this problem.

The direct dynamic solution requires the solution of direct kinematics. Similar to the dynamics, there exist many studies on the kinematics. In general, there are two approaches, analytical and numerical, for kinematics solution. Analytical approaches exist for solving the DKP of Gough–Stewart robots such as 'the elimination method' [19–21] and 'the Gröebner basis method' [22–24]. These methods are not useful for real-time control and simulation due to the need to determine the acceptable solution among the many available solutions [25–28]. Moreover, in general, DKP does not admit closed-form solutions, and therefore, numerical approaches need to be adopted [28,29]. There exist convenient numerical iterative methods which start the search from an initial guess and converge to one of the direct kinematics solutions. Newton's method is widely employed in the DKP of parallel robots [28–30]. However, the initial guess plays an important role on the number of iterations needed for finding a solution and even the convergence of the process. Pratik and Lam [30] presented a novel strategy for providing an appropriate initial guess for a standard Newton–Raphson technique using neural network.

In this paper, the principle of virtual work is employed for the first time, for solving both the inverse and direct dynamics of a Gough–Stewart parallel manipulator. Section 2 covers the Gough–Stewart platform description and kinematical parameters. In Sects. 3 and 4, the moving platform velocity is discussed and concept of inverse and direct link Jacobian matrices is used to relate the motion between joints (active and/or passive) and actuators velocity vector. Next, in Sect. 5, the moving platform accelerations and in Sect. 6 the link accelerations are analyzed. Section 7 covers resultant wrench and inertia of the moving platform. In Sect. 8, the dynamics equations of motion are formulated by employing the concept of virtual work. In Sect. 9, improved hybrid strategy is applied for solving the DKP of Gough–Stewart platform. Two examples, covering the direct and inverse dynamics, are also presented. In the first example, a robot trajectory is selected, and the inverse dynamics using the virtual work is solved to obtain required motor torques. Results are next verified with commercial dynamics software. In the second example, the input of the direct dynamics is compared with the output of the inverse dynamics. To do this, another trajectory is first selected and the inverse dynamics is used to obtain the required motor torques. These motor torques are next used as input for the direct dynamics formulation, and a resulting MP trajectory is obtained. This section also covers comparison between Lagrange–Euler formulation and the proposed dynamics method.

2 Inverse position analysis

Consider Fig. 1a. Frame {T} and frame {B} are attached to the moving platform, MP, and fixed base, respectively.

The rotation matrix, ${}^{\mathrm{B}}_{\mathrm{T}}\mathbf{R}$, consists of three Euler angles θ, φ and λ rotated about x, y and z-axes, respectively and can be defined as

$$
\begin{aligned}
{}^{\mathrm{B}}_{\mathrm{T}}\mathbf{R} &= \mathbf{R}(x,\theta)\mathbf{R}(y,\varphi)\mathbf{R}(z,\lambda) \\
&= \begin{bmatrix} \mathrm{c}\lambda\,\mathrm{c}\varphi & -\mathrm{c}\varphi\mathrm{s}\lambda & \mathrm{s}\varphi \\ \mathrm{c}\theta\,\mathrm{s}\lambda+\mathrm{c}\lambda\,\mathrm{s}\varphi\,\mathrm{s}\theta & \mathrm{c}\lambda\,\mathrm{c}\theta-\mathrm{s}\lambda\,\mathrm{s}\varphi\,\mathrm{s}\theta & -\mathrm{c}\varphi\,\mathrm{s}\theta \\ \mathrm{s}\lambda\,\mathrm{s}\theta-\mathrm{c}\lambda\,\mathrm{c}\theta\,\mathrm{s}\varphi & \mathrm{c}\lambda\,\mathrm{s}\theta+\mathrm{c}\theta\,\mathrm{s}\lambda\,\mathrm{s}\varphi & \mathrm{c}\varphi\,\mathrm{c}\theta \end{bmatrix}
\end{aligned} \tag{1}
$$

where c and s represent cosine and sine, respectively. Therefore, to express an arbitrary ${}^{\mathrm{T}}\boldsymbol{\vartheta}$, defined in {T} to {B}, we have

$$
{}^{\mathrm{B}}\boldsymbol{\vartheta} = {}^{\mathrm{B}}_{\mathrm{T}}\mathbf{R}\,{}^{\mathrm{T}}\boldsymbol{\vartheta} \tag{2}
$$

In this paper, a leading superscript represents the coordinate frame in which the vector is referenced. Additionally, bold lower and upper case lettering designate vectors and matrices, respectively. For brevity, the superscript "B" denoting the frame {B} in which vectors are defined is eliminated.

Figure 1b represents vectors and coordinate frames used for the kinematic problem of the 6-UPS manipulator. For each kinematic chain, a closed vector-loop equation can be written as follows

$$
\mathbf{a}_i + \mathbf{q}_i^{\mathrm{ac}} = {}^{\mathrm{B}}_{\mathrm{T}}\mathbf{R}\,{}^{\mathrm{T}}\mathbf{b}_i + \mathbf{p} \quad \text{for } i = 1,\ldots,6 \tag{3}
$$

where ${}^{\mathrm{B}}_{\mathrm{T}}\mathbf{R}$ is a rotation matrix to transfer a vector defined in {T} to {B}. Vectors $\mathbf{a}_i$, ${}^{\mathrm{T}}\mathbf{b}_i$ and $\mathbf{p}$ denote position of point U_i relative to frame {B}, position of point S_i relative to frame {T} and the translation vector of the tip, point P, respectively. The constraint equations, Eq. (3), is a system of nonlinear algebraic equations as $\mathbf{F}(\mathbf{q}) = \mathbf{0}$, where $\mathbf{q} = \left\{q_1^{\mathrm{ac}},\ldots,q_6^{\mathrm{ac}},x_{\mathrm{P}},y_{\mathrm{P}},z_{\mathrm{P}},\theta,\varphi,\lambda\right\}$. The actuated joints

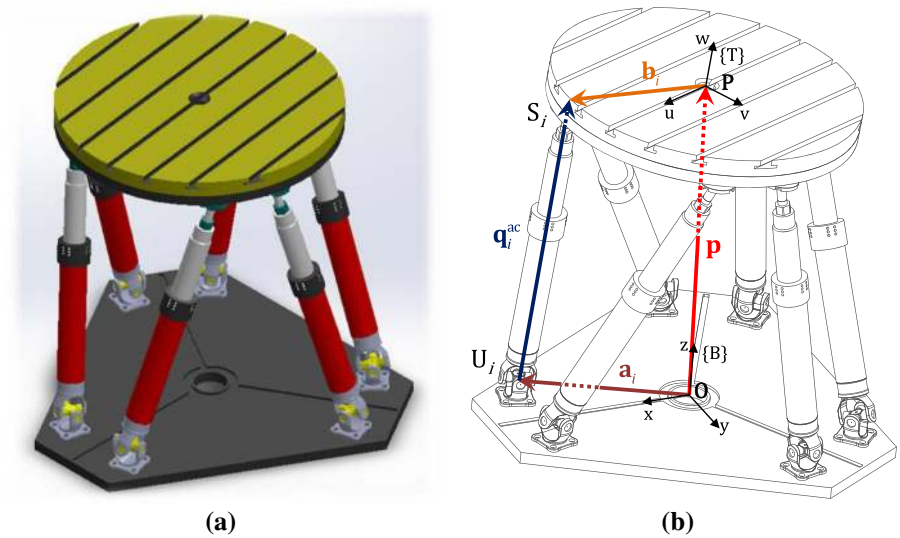

Fig. 1 **a** The physical model and **b** a closed loop vector for *i*th leg of the 6-UPS parallel robot

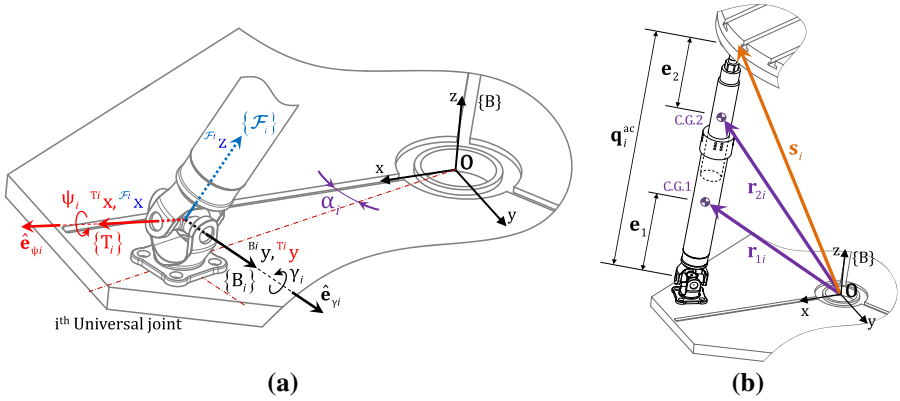

Fig. 2 **a** Local coordinates frames for *i*th passive universal joint, **b** position vectors and dimensional parameters of *i*th actuated limb

values, q_i^{ac}, and unit vectors along the actuated prismatic joints, $\hat{\mathbf{q}}_i^{ac}$, can be obtained using Eq. (3) as follows

$$q_i^{ac} = \left\| {}^{B}_{T}\mathbf{R}^{T}\mathbf{b}_i + \mathbf{p} - \mathbf{a}_i \right\|$$

$$\hat{\mathbf{q}}_i^{ac} = \frac{1}{q_i^{ac}}\left({}^{B}_{T}\mathbf{R}^{T}\mathbf{b}_i + \mathbf{p} - \mathbf{a}_i\right) \quad \text{for} \quad i = 1, \ldots, 6 \tag{4}$$

As shown in Fig. 2b, the actuated prismatic joints include two cylindrical parts. The center of gravity positions of these parts can be calculated as follows

$$\mathbf{r}_{1i} = \mathbf{a}_i + e_1\hat{\mathbf{q}}_i^{ac} \quad \text{and} \quad \mathbf{r}_{2i} = \mathbf{a}_i + \left(q_i^{ac} - e_2\right)\hat{\mathbf{q}}_i^{ac} \quad \text{for} \quad i = 1, \ldots, 6 \tag{5}$$

Furthermore, to calculate the rotation values of U-joint, the following method is utilized. As shown in Fig. 1a, the rotation matrix, which transfers local moving frame $\{\mathcal{F}_i\}$ to fixed frame $\{B\}$ for *i*th passive U-joint, can be obtained as

$${}^{B}_{\mathcal{F}i}\mathbf{R} = \mathbf{R}(z, \alpha_i)\,\mathbf{R}(y, \gamma_i)\,\mathbf{R}(x, \psi_i) = \begin{bmatrix} c\alpha_i c\gamma_i & -s\alpha_i c\psi_i + c\alpha_i s\gamma_i s\psi_i & s\alpha_i s\psi_i + c\alpha_i s\gamma_i c\psi_i \\ s\alpha_i c\gamma_i & c\alpha_i c\psi_i + s\alpha_i s\gamma_i s\psi_i & -c\alpha_i s\psi_i + s\alpha_i s\gamma_i c\psi_i \\ -s\gamma_i & c\gamma_i s\psi_i & c\gamma_i c\psi_i \end{bmatrix} \tag{6}$$

where α_i is a constant value and is illustrated in Fig. 2a. Using Eq. (6), we have

$$\hat{\mathbf{q}}_i^{ac} = {}^{B}_{\mathcal{F}i}\mathbf{R}\,{}^{\mathcal{F}i}\hat{\mathbf{q}}_i^{ac} = \begin{Bmatrix} s\alpha_i s\psi_i + c\alpha_i s\gamma_i c\psi_i \\ -c\alpha_i s\psi_i + s\alpha_i s\gamma_i c\psi_i \\ c\gamma_i c\psi_i \end{Bmatrix} = \begin{Bmatrix} \hat{q}_{ix}^{ac} \\ \hat{q}_{iy}^{ac} \\ \hat{q}_{iz}^{ac} \end{Bmatrix} \quad \text{for} \quad i = 1, \ldots, 6 \tag{7}$$

where ${}^{\mathcal{F}i}\hat{\mathbf{q}}_i^{ac} = \left\{0\ 0\ 1\right\}^{T}$. By comparing Eqs. (4) and (7) and solving the inverse kinematics problem as well

as solving Eq. (4), the rotation angles for ith passive U-joint, i.e., γ_i and ψ_i, can be obtained as

$$\mathrm{s}\psi_i = \mathrm{s}\alpha_i\, \hat{\mathrm{q}}_{ix}^{\mathrm{ac}} - \mathrm{c}\alpha_i\, \hat{\mathrm{q}}_{iy}^{\mathrm{ac}} \tag{8}$$

and

$$\mathrm{s}\gamma_i \mathrm{c}\psi_i = \mathrm{c}\alpha_i \hat{\mathrm{q}}_{ix}^{\mathrm{ac}} + \mathrm{s}\alpha_i \hat{\mathrm{q}}_{iy}^{\mathrm{ac}} \quad \text{and} \quad \mathrm{c}\gamma_i \mathrm{c}\psi_i = \hat{\mathrm{q}}_{iz}^{\mathrm{ac}}$$
$$\rightarrow \tan\gamma_i = \frac{\left(\mathrm{c}\alpha_i \hat{\mathrm{q}}_{ix}^{\mathrm{ac}} + \mathrm{s}\alpha_i \hat{\mathrm{q}}_{iy}^{\mathrm{ac}}\right)}{\hat{\mathrm{q}}_{iz}^{\mathrm{ac}}} \tag{9}$$

3 Inverse and direct velocity analysis of the moving platform

The velocity vector equations are found by time differentiating both sides of Eq. (3) as

$$\dot{\mathrm{q}}_i^{\mathrm{ac}}\, \hat{\mathbf{q}}_i^{\mathrm{ac}} + \mathrm{q}_i^{\mathrm{ac}}\, \boldsymbol{\omega}_{\mathrm{Leg},i} \times \hat{\mathbf{q}}_i^{\mathrm{ac}} = \boldsymbol{v}_{\mathrm{P}} + \boldsymbol{\omega}_{\mathrm{MP}} \times \mathbf{b}_i \quad \text{for } i = 1, \ldots, 6 \tag{10}$$

where $\boldsymbol{v}_{\mathrm{P}} = \left\{ \dot{\mathrm{x}}_{\mathrm{P}}\ \dot{\mathrm{y}}_{\mathrm{P}}\ \dot{\mathrm{z}}_{\mathrm{P}} \right\}^{\mathrm{T}}$ and $\boldsymbol{\omega}_{\mathrm{MP}} = \left\{ \omega_x\ \omega_y\ \omega_z \right\}^{\mathrm{T}}$ denote Cartesian velocity vector of the tip, point P, and angular velocity vector of the MP, respectively. The velocity of ith S-joint, point S_i, can be written in terms of translational and rotational velocities of the MP as follows

$$\boldsymbol{v}_{\mathrm{S}i} = \boldsymbol{v}_{\mathrm{P}} + \boldsymbol{\omega}_{\mathrm{MP}} \times \mathbf{b}_i \qquad \text{for } i = 1, \ldots, 6 \tag{11}$$

where $\mathbf{b}_i = \left\{ b_{ix}\ b_{iy}\ b_{iz} \right\}^{\mathrm{T}}$. For two arbitrary vectors $\mathbf{a}$ and $\mathbf{c}$, we can write

$$\mathbf{a} \times \mathbf{c} = \varepsilon_{ijk} a_j c_k \tag{12}$$

where j and k are dummy indices and ε_{ijk} is the *permutation symbol*. Therefore, to obtain inverse velocity relation in matrix form, Eq. (11) can be rewritten as

$$\boldsymbol{v}_{\mathrm{S}i} = \mathbf{J}_{\mathrm{MP}i}\, \mathbf{t}_{\mathrm{MP}} \quad \text{for } i = 1, \ldots, 6 \tag{13}$$

where $\mathbf{t}_{\mathrm{MP}} = \left\{ \boldsymbol{v}_{\mathrm{P}}^{\mathrm{T}}\ \boldsymbol{\omega}_{\mathrm{MP}}^{\mathrm{T}} \right\}^{\mathrm{T}}$ represent the twist vector of the MP and $\boldsymbol{v}_{\mathrm{S}i} = \left\{ \dot{\mathrm{x}}_{\mathrm{S}i}\ \dot{\mathrm{y}}_{\mathrm{S}i}\ \dot{\mathrm{z}}_{\mathrm{S}i} \right\}^{\mathrm{T}}$ is velocity vector of the ith S-joint as well as $\mathbf{J}_{\mathrm{MP}i}$ is the 3×6 matrix which maps the twist vector of the MP to the ith S-joint velocity. The matrix $\mathbf{J}_{\mathrm{MP}i}$ can be found in "Appendix 1." Furthermore, we know that

$$\dot{\mathrm{q}}_i^{\mathrm{ac}} = {}^{\mathcal{F}i}\boldsymbol{v}_{\mathrm{S}i} \cdot {}^{\mathcal{F}i}\hat{\mathbf{q}}_i^{\mathrm{ac}} = {}^{\mathcal{F}i}\dot{\mathrm{z}}_{\mathrm{S}i} \quad \text{for } i = 1, \ldots, 6 \tag{14}$$

where ${}^{\mathcal{F}i}\dot{\mathrm{z}}_{\mathrm{S}i}$ is the velocity of ith S-joint along the z-axis of local moving frame $\{\mathcal{F}i\}$ which can be represented as the ith actuator velocity. Note that, $\left({}^{\mathrm{B}}_{\mathcal{F}i}\mathbf{R}\right)^{-1} = \left({}^{\mathrm{B}}_{\mathcal{F}i}\mathbf{R}\right)^{\mathrm{T}} = {}^{\mathcal{F}i}_{\mathrm{B}}\mathbf{R}$. Therefore, multiplying the both sides of Eq. (13) by ${}^{\mathcal{F}i}_{\mathrm{B}}\mathbf{R}$ yield

$${}^{\mathcal{F}i}\boldsymbol{v}_{\mathrm{S}i} = {}^{\mathcal{F}i}_{\mathrm{B}}\mathbf{R}\, \boldsymbol{v}_{\mathrm{S}i} = {}^{\mathcal{F}i}_{\mathrm{B}}\mathbf{R}\, \mathbf{J}_{\mathrm{MP}i}\, \mathbf{t}_{\mathrm{MP}} = {}^{\mathcal{F}i}\mathbf{J}_{\mathrm{MP}i}\mathbf{t}_{\mathrm{MP}} \quad \text{for } i = 1, \ldots, 6 \tag{15}$$

By comparing Eqs. (14) and (15) as well as selecting the z component of velocity vector ${}^{\mathcal{F}i}\boldsymbol{v}_{\mathrm{S}i}$, the inverse velocity relation for ith leg of the 6-UPS parallel robot can be obtained as

$$\dot{\mathrm{q}}_i^{\mathrm{ac}} = {}^{\mathcal{F}i}\dot{\mathrm{z}}_{\mathrm{S}i} = {}^{\mathcal{F}i}\mathbf{J}_{\mathrm{MP}i(3\times 1-6)}\mathbf{t}_{\mathrm{MP}} \quad \text{for } i = 1, \ldots, 6 \tag{16}$$

where ${}^{\mathcal{F}i}\mathbf{J}_{\mathrm{MP}i(k\times 1-6)}$ is the kth row of matrix ${}^{\mathcal{F}i}\mathbf{J}_{\mathrm{MP}i}$. The *overall inverse velocity* relation for the robot can be obtained in familiar matrix form as

$$\dot{\mathbf{q}}^{\mathrm{ac}} = \mathbf{J}_{\mathrm{MP}}\, \mathbf{t}_{\mathrm{MP}} \tag{17}$$

where $\dot{\mathbf{q}}^{\mathrm{ac}} = \{\dot{\mathrm{q}}_1^{\mathrm{ac}}, \ldots, \dot{\mathrm{q}}_6^{\mathrm{ac}}\}$ represents the linear actuated joint velocities. Furthermore, $\mathbf{J}_{\mathrm{MP}}$ is a 6×6 square matrix called *inverse Jacobian matrix* of the robot. Using Eq. (16), Jacobian matrix $\mathbf{J}_{\mathrm{MP}}$ can be obtained. This matrix can be found in "Appendix 1." Note that the angular velocity of MP, $\boldsymbol{\omega}_{\mathrm{MP}}$ can be specified as function of three Euler angular velocities, $\dot{\theta}$, $\dot{\varphi}$, and $\dot{\lambda}$ (see "Appendix 4").

Clearly, to obtain the *overall direct velocity* relation which maps the ith actuated joint velocities, $\dot{\mathrm{q}}_i^{\mathrm{ac}}$, to the twist vector of the MP, $\mathbf{t}_{\mathrm{MP}}$, Eq. (17) can be rewritten as follows

$$\mathbf{t}_{\mathrm{MP}} = \mathbf{J}_{\mathrm{MP}}^{-1}\, \dot{\mathbf{q}}^{\mathrm{ac}} \tag{18}$$

where $\mathbf{J}_{\mathrm{MP}}^{-1}$ is a 6×6 square matrix called *direct Jacobian matrix* of the 6-UPS parallel robot.

4 Inverse and direct link Jacobian matrices

The velocity vector of ith S-joint in $\{\mathcal{F}i\}$ can be written in terms of the ith actuator velocity and angular velocity of the ith limb of the robot using Eq. (10) as follows

$${}^{\mathcal{F}i}\boldsymbol{v}_{\mathrm{S}i} = {}^{\mathcal{F}i}_{\mathrm{B}}\mathbf{R}\, \boldsymbol{v}_{\mathrm{S}i} = \dot{\mathrm{q}}_i^{\mathrm{ac}}\, {}^{\mathcal{F}i}\hat{\mathbf{q}}_i^{\mathrm{ac}} + \mathrm{q}_i^{\mathrm{ac}}\, {}^{\mathcal{F}i}\boldsymbol{\omega}_{\mathrm{Leg},i} \times {}^{\mathcal{F}i}\hat{\mathbf{q}}_i^{\mathrm{ac}} \quad \text{for } i = 1, \ldots, 6 \tag{19}$$

Furthermore, as illustrated in Fig. 2a, the ith leg of robot can rotate around the y-axis of fixed frame $\{B_i\}$ by γ_i. Then it rotates around the x-axis of moving frame $\{T_i\}$ by ψ_i. Since these two rotation axes are not always perpendicular to the leg, it means that we cannot state that the ith leg of 6-UPS robot does not have spin about z-axis of frame $\{\mathcal{F}i\}$. Therefore, we can claim that the statement of ${}^{\mathcal{F}i}\boldsymbol{\omega}_{\mathrm{Leg},i} = \left({}^{\mathcal{F}i}\hat{\mathbf{q}}_i^{\mathrm{ac}} \times {}^{\mathcal{F}i}\boldsymbol{v}_{\mathrm{S}i}\right)/q_i^{\mathrm{ac}}$ commonly used in previous literature [15] is not always right. This formulation is only a good approximation and does not produce the accurate results. This is because, the angular velocity of ith leg in its local frame $\{\mathcal{F}_i\}$, ${}^{\mathcal{F}i}\boldsymbol{\omega}_{\mathrm{Leg},i}$, cannot always be obtained by using cross product of both sides of Eq. (19) with the unit vector ${}^{\mathcal{F}i}\hat{\mathbf{q}}_i^{\mathrm{ac}}$. In the present paper, the angular velocity of ith leg is obtained using the angular velocities of the two consecutive R-joints of the ith U-joint. Therefore, considering Fig. 2a, we obtain the angular velocity of ith leg in $\{\mathcal{F}_i\}$ using the ith U-joint angular velocities as follows

$$ {}^{\mathcal{F}i}\boldsymbol{\omega}_{\mathrm{Leg},i} = \dot{\gamma}_i\, {}^{\mathcal{F}i}\hat{\mathbf{e}}_{\gamma i} + \dot{\psi}\, {}^{\mathcal{F}i}\hat{\mathbf{e}}_{\psi i} \quad \text{for} \quad i = 1, \ldots, 6 \tag{20} $$

where

$$ {}^{\mathcal{F}i}\hat{\mathbf{e}}_{\gamma i} = \mathbf{R}^{\mathrm{T}}(x, \psi_i)\, \mathbf{R}^{\mathrm{T}}(y, \gamma_i) \begin{Bmatrix} 0 \\ 1 \\ 0 \end{Bmatrix}, $$

$$ {}^{\mathcal{F}i}\hat{\mathbf{e}}_{\psi i} = \mathbf{R}^{\mathrm{T}}(x, \psi_i) \begin{Bmatrix} 1 \\ 0 \\ 0 \end{Bmatrix} \quad \text{for} \quad i = 1, \ldots, 6 \tag{21} $$

where $\dot{\gamma}_i$ and $\dot{\psi}_i$ are the angular velocities and ${}^{\mathcal{F}i}\hat{\mathbf{e}}_{\gamma i}$ and ${}^{\mathcal{F}i}\hat{\mathbf{e}}_{\psi i}$ represent the unit vectors along rotation axes of the two R-joints of ith passive U-joint (see Fig. 2a). Equation (21) can be rewritten in matrix form as follows

$$ \begin{aligned} {}^{\mathcal{F}i}\boldsymbol{\omega}_{\mathrm{Leg},i} &= {}^{\mathcal{F}i}\mathbf{k}_{\mathrm{U}i} \begin{Bmatrix} \dot{\gamma}_i \\ \dot{\psi}_i \end{Bmatrix} \\ &= \begin{Bmatrix} \dot{\psi}_i \\ \dot{\gamma}_i \cos(\psi_i) \\ -\dot{\gamma}_i \sin(\psi_i) \end{Bmatrix} \quad \text{for} \quad i = 1, \ldots, 6 \end{aligned} \tag{22} $$

where ${}^{\mathcal{F}i}\mathbf{k}_{\mathrm{U}i}$ is Jacobian matrix which maps the joint angular velocities of ith passive U-joint to the angular velocity of ith leg, and it can be expressed as follows

$$ {}^{\mathcal{F}i}\mathbf{k}_{\mathrm{U}i} = \left[{}^{\mathcal{F}i}\hat{\mathbf{e}}_{\gamma i}\ {}^{\mathcal{F}i}\hat{\mathbf{e}}_{\psi i} \right]_{3\times 2} \quad \text{for} \quad i = 1, \ldots, 6 \tag{23} $$

To obtain values of $\dot{\gamma}_i$ and $\dot{\psi}_i$, we can cross product both sides of Eq. (19) with unit vector ${}^{\mathcal{F}i}\hat{\mathbf{q}}_i^{\mathrm{ac}}$. This yield

$$ \begin{aligned} &{}^{\mathcal{F}i}\hat{\mathbf{q}}_i^{\mathrm{ac}} \times \left({}^{\mathcal{F}i}\boldsymbol{\omega}_{\mathrm{Leg},i} \times {}^{\mathcal{F}i}\hat{\mathbf{q}}_i^{\mathrm{ac}}\right) \\ &= \left({}^{\mathcal{F}i}\hat{\mathbf{q}}_i^{\mathrm{ac}} \times {}^{\mathcal{F}i}\boldsymbol{v}_{\mathrm{S}i}\right)/\mathrm{q}_i^{\mathrm{ac}} \quad \text{for} \quad i = 1, \ldots, 6 \end{aligned} \tag{24} $$

Consider

$$ \mathbf{a} \times (\mathbf{b} \times \mathbf{c}) = (\mathbf{a} \cdot \mathbf{c})\,\mathbf{b} - (\mathbf{a} \cdot \mathbf{b})\,\mathbf{c} \quad \text{and} \quad \mathbf{a} \times \mathbf{b} = -\mathbf{b} \times \mathbf{a} \tag{25} $$

Therefore, Eq. (24) can be simplified using Eq. (22) as

$$ \begin{aligned} \begin{Bmatrix} {}^{\mathcal{F}i}\omega_{\mathrm{Leg},ix} \\ {}^{\mathcal{F}i}\omega_{\mathrm{Leg},iy} \\ 0 \end{Bmatrix} &= \begin{Bmatrix} \dot{\psi}_i \\ \dot{\gamma}_i \cos(\psi_i) \\ 0 \end{Bmatrix} \\ &= \left({}^{\mathcal{F}i}\hat{\mathbf{q}}_i^{\mathrm{ac}} \times {}^{\mathcal{F}i}\boldsymbol{v}_{\mathrm{S}i}\right)/\mathrm{q}_i^{\mathrm{ac}} \quad \text{for} \quad i = 1, \ldots, 6 \end{aligned} \tag{26} $$

Substituting ${}^{\mathcal{F}i}\boldsymbol{v}_{\mathrm{S}i}$ from Eqs. (15) in (26), yields

$$ \begin{aligned} \dot{\psi}_i &= \frac{-1}{\mathrm{q}_i^{\mathrm{ac}}} \left({}^{\mathcal{F}i}\mathbf{J}_{\mathrm{MP}i(2\times 1-6)}\mathbf{t}_{\mathrm{MP}}\right) \\ \dot{\gamma}_i &= \frac{1}{\mathrm{q}_i^{\mathrm{ac}} \cos(\psi_i)} \left({}^{\mathcal{F}i}\mathbf{J}_{\mathrm{MP}i\ (1\times 1-6)}\mathbf{t}_{\mathrm{MP}}\right) \\ &\quad \text{for} \quad i = 1, \ldots, 6 \end{aligned} \tag{27} $$

Finally, substituting values of $\dot{\gamma}_i$ and $\dot{\psi}_i$ from Eq. (27) in Eq. (22) yield

$$ {}^{\mathcal{F}i}\boldsymbol{\omega}_{\mathrm{Leg},i} = \mathbf{J}_{\omega i}\mathbf{t}_{\mathrm{MP}} \quad \text{for} \quad i = 1, \ldots, 6 \tag{28} $$

where $\mathbf{J}_{\omega i}$ is a 3×6 matrix and can be found in "Appendix 1." The mass centers' velocities of the actuators' cylinder and piston can be derived by time differentiating from Eq. (5). This yields

$$ \begin{aligned} {}^{\mathcal{F}i}\boldsymbol{v}_{\mathrm{C.G.1}i} &= {}^{\mathcal{F}i}_{\mathrm{B}}\mathbf{R}_{\mathrm{U}i}\boldsymbol{v}_{\mathrm{C.G.1}i} \\ &= \mathrm{e}_1\, {}^{\mathcal{F}i}\boldsymbol{\omega}_{\mathrm{Leg},i} \times {}^{\mathcal{F}i}\hat{\mathbf{q}}_i^{\mathrm{ac}} \\ {}^{\mathcal{F}i}\boldsymbol{v}_{\mathrm{C.G.2}i} &= {}^{\mathcal{F}i}_{\mathrm{B}}\mathbf{R}_{\mathrm{U}i}\boldsymbol{v}_{\mathrm{C.G.2}i} = \dot{\mathbf{q}}^{\mathrm{ac}}\, {}^{\mathcal{F}i}\hat{\mathbf{q}}_i^{\mathrm{ac}} \\ &\quad + \left(q_i^{\mathrm{ac}} - e_2\right) {}^{\mathcal{F}i}\boldsymbol{\omega}_{\mathrm{Leg},i} \times {}^{\mathcal{F}i}\hat{\mathbf{q}}_i^{\mathrm{ac}} \\ &\quad \text{for} \quad i = 1, \ldots, 6 \end{aligned} \tag{29} $$

Using Eq. (28), term ${}^{\mathcal{F}i}\boldsymbol{\omega}_{\mathrm{Leg},i} \times {}^{\mathcal{F}i}\hat{\mathbf{q}}_i^{\mathrm{ac}}$ can be simplified as follows

$$ \begin{aligned} &{}^{\mathcal{F}i}\boldsymbol{\omega}_{\mathrm{Leg},i} \times {}^{\mathcal{F}i}\hat{\mathbf{q}}_i^{\mathrm{ac}} \\ &= \frac{1}{q_i^{\mathrm{ac}}} \begin{bmatrix} {}^{\mathcal{F}i}\mathbf{J}_{\mathrm{MP}i(1-2\times 1-6)} \\ \mathbf{0}_{1\times 6} \end{bmatrix}_{3\times 6} \mathbf{t}_{\mathrm{MP}} \quad \text{for} \quad i = 1, \ldots, 6 \end{aligned} \tag{30} $$

Substituting Eqs. (30) into (29) will yield

$$ \begin{aligned} {}^{\mathcal{F}i}\boldsymbol{v}_{\mathrm{C.G.1}i} &= \mathbf{J}_{v1,i}\mathbf{t}_{\mathrm{MP}} \\ {}^{\mathcal{F}i}\boldsymbol{v}_{\mathrm{C.G.2}i} &= \mathbf{J}_{v2,i}\mathbf{t}_{\mathrm{MP}} \quad \text{for} \quad i = 1, \ldots, 6 \end{aligned} \tag{31} $$

where $\mathbf{J}_{v1,i}$ and $\mathbf{J}_{v2,i}$ are 3×6 matrices and can be found in "Appendix 1." Equations (28) and (31) are called the *inverse link velocity relations*. By combining these equations, the *overall inverse link velocity relations* are obtained as follows

$$\begin{aligned}{}^{\mathcal{F}i}\mathbf{t}_{\mathrm{cyl},i} &= \mathbf{J}_{\mathrm{inv,cyl},i}\,\mathbf{t}_{\mathrm{MP}} \quad \text{for} \quad i=1,\ldots,6\\ {}^{\mathcal{F}i}\mathbf{t}_{\mathrm{pis},i} &= \mathbf{J}_{\mathrm{inv,pis},i}\,\mathbf{t}_{\mathrm{MP}} \quad \text{for} \quad i=1,\ldots,6\end{aligned} \tag{32}$$

where ${}^{\mathcal{F}i}\mathbf{t}_{\mathrm{cyl},i} = \left\{ {}^{\mathcal{F}i}\boldsymbol{v}^{\mathrm{T}}_{\mathrm{C.G.1}i}\ {}^{\mathcal{F}i}\boldsymbol{\omega}^{\mathrm{T}}_{\mathrm{Leg},i} \right\}^{\mathrm{T}}$ and ${}^{\mathcal{F}i}\mathbf{t}_{\mathrm{pis},i} = \left\{ {}^{\mathcal{F}i}\boldsymbol{v}^{\mathbf{T}}_{\mathrm{C.G.2}i}\ {}^{\mathcal{F}i}\boldsymbol{\omega}^{\mathrm{T}}_{\mathrm{Leg},i} \right\}^{\mathrm{T}}$ represent the twist vectors for cylinder and piston of the ith robot's leg, respectively. Furthermore, $\mathbf{J}_{\mathrm{inv,cyl},i} = \left[\mathbf{J}^{\mathbf{T}}_{v1,i}\ \mathbf{J}^{\mathrm{T}}_{\omega i}\right]^{\mathrm{T}}$ and $\mathbf{J}_{\mathrm{inv,pis},i} = \left[\mathbf{J}^{\mathbf{T}}_{v2,i}\ \mathbf{J}^{\mathrm{T}}_{\omega i}\right]^{\mathrm{T}}$ denote the *overall inverse link Jacobian matrices* which map the MP's twist vector to the twist vectors of cylinder and piston of the ith robot's leg, respectively. Additionally, Eq. (18) is used to derive the link velocity relations in terms of the actuated joint velocities, $\dot{\mathbf{q}}^{\mathrm{ac}}$. Substituting Eq. (18) into Eqs. (28) and (31) yields

$$\begin{aligned}{}^{\mathcal{F}i}\boldsymbol{\omega}_{\mathrm{Leg},i} &= \mathbf{J}_{\omega i}\mathbf{J}^{-1}_{\mathrm{MP}}\dot{\mathbf{q}}^{\mathrm{ac}}\\ {}^{\mathcal{F}i}\boldsymbol{v}_{\mathrm{C.G.1}i} &= \mathbf{J}_{v1,i}\mathbf{J}^{-1}_{\mathrm{MP}}\dot{\mathbf{q}}^{\mathrm{ac}}\\ {}^{\mathcal{F}i}\boldsymbol{v}_{\mathrm{C.G.2}i} &= \mathbf{J}_{v2,i}\mathbf{J}^{-1}_{\mathrm{MP}}\dot{\mathbf{q}}^{\mathrm{ac}} \quad \text{for} \quad i=1,\ldots,6\end{aligned} \tag{33}$$

Additionally, obtaining the twist vectors of each link of the robot in terms of the actuated joint velocities is necessary to derive the direct dynamics relations. Therefore, the overall direct link velocity relations are derived by combining Eq. (33) as follows

$$\begin{aligned}{}^{\mathcal{F}i}\mathbf{t}_{\mathrm{cyl},i} &= \mathbf{J}_{\mathrm{dir,cyl},i}\,\dot{\mathbf{q}}^{\mathrm{ac}}\\ {}^{\mathcal{F}i}\mathbf{t}_{\mathrm{pis},i} &= \mathbf{J}_{\mathrm{dir,pis},i}\,\dot{\mathbf{q}}^{\mathrm{ac}} \quad \text{for} \quad i=1,\ldots,6\end{aligned} \tag{34}$$

where, $\mathbf{J}_{\mathrm{dir,cyl},i} = \mathbf{J}_{\mathrm{inv,cyl},i}\mathbf{J}^{-1}_{\mathrm{MP}}$ and $\mathbf{J}_{\mathrm{dir,pis},i} = \mathbf{J}_{\mathrm{inv,pis},i}\ \mathbf{J}^{-1}_{\mathrm{MP}}$ denote the *overall direct link Jacobian matrices* which map the actuators' velocity vector to the twist vectors of cylinder and piston of the ith robot's leg, respectively.

5 The moving platform acceleration analysis

By taking the time derivative of both sides of Eq. (10), the acceleration relation of the ith robot's leg can be derived as follows

$$\begin{aligned}&\ddot{\mathrm{q}}^{\mathrm{ac}}_i\hat{\mathbf{q}}^{\mathrm{ac}}_i + 2\dot{\mathrm{q}}^{\mathrm{ac}}_i\boldsymbol{\omega}_{\mathrm{Leg},i}\times\hat{\mathbf{q}}^{\mathrm{ac}}_i + \mathrm{q}^{\mathrm{ac}}_i\dot{\boldsymbol{\omega}}_{\mathrm{Leg},i}\times\hat{\mathbf{q}}^{\mathrm{ac}}_i\\ &\quad + \mathrm{q}^{\mathrm{ac}}_i\boldsymbol{\omega}_{\mathrm{Leg},i}\times\left(\boldsymbol{\omega}_{\mathrm{Leg},i}\times\hat{\mathbf{q}}^{\mathrm{ac}}_i\right)\\ &= \dot{\boldsymbol{v}}_{\mathrm{P}} + \dot{\boldsymbol{\omega}}_{\mathrm{MP}}\times\mathbf{b}_i + \boldsymbol{\omega}_{\mathrm{MP}}\times(\boldsymbol{\omega}_{\mathrm{MP}}\times\mathbf{b}_i)\\ &\quad \text{for } i=1,\ldots,6\end{aligned} \tag{35}$$

where $\dot{\boldsymbol{v}}_{\mathrm{P}} = \{\ddot{\mathrm{x}}_{\mathrm{P}}\ \ddot{\mathrm{y}}_{\mathrm{P}}\ \ddot{\mathrm{z}}_{\mathrm{P}}\}^{\mathrm{T}}$ and $\dot{\boldsymbol{\omega}}_{\mathrm{MP}} = \{\dot{\omega}_x\ \dot{\omega}_y\ \dot{\omega}_z\}^{\mathrm{T}}$ denote Cartesian acceleration vector of the tip, point P, and angular acceleration vector of the MP, respectively. The acceleration of ith S-joint, point S_i, can be written in terms of velocities and accelerations of the MP as follows

$$\begin{aligned}\dot{\boldsymbol{v}}_{\mathrm{S}i} &= \dot{\boldsymbol{v}}_{\mathrm{P}} + \dot{\boldsymbol{\omega}}_{\mathrm{MP}}\times\mathbf{b}_i + \boldsymbol{\omega}_{\mathrm{MP}}\times(\boldsymbol{\omega}_{\mathrm{MP}}\times\mathbf{b}_i)\\ &\quad \text{for} \quad i=1,\ldots,6\end{aligned} \tag{36}$$

By considering Eq. (25), the Eq. (36) can be rewritten as

$$\begin{aligned}\dot{\boldsymbol{v}}_{\mathrm{S}i} &= \dot{\boldsymbol{v}}_{\mathrm{P}} + \dot{\boldsymbol{\omega}}_{\mathrm{MP}}\times\mathbf{b}_i + (\boldsymbol{\omega}_{\mathrm{MP}}\cdot\mathbf{b}_i)\boldsymbol{\omega}_{\mathrm{MP}}\\ &\quad -(\boldsymbol{\omega}_{\mathrm{MP}}\cdot\boldsymbol{\omega}_{\mathrm{MP}})\mathbf{b}_i \quad \text{for} \quad i=1,\ldots,6\end{aligned} \tag{37}$$

Therefore, Eq. (37) can be rewritten in matrix form as

$$\dot{\boldsymbol{v}}_{\mathrm{S}i} = \mathbf{J}_{\mathrm{MP}i}\dot{\mathbf{t}}_{\mathrm{MP}} + \mathbf{N}_i\boldsymbol{\omega}_{\mathrm{MP}} + \mathbf{m}_i \quad \text{for} \quad i=1,\ldots,6 \tag{38}$$

where $\dot{\mathbf{t}}_{\mathrm{MP}} = \{\dot{\boldsymbol{v}}^{\mathrm{T}}_{\mathrm{P}}\ \dot{\boldsymbol{\omega}}^{\mathrm{T}}_{\mathrm{MP}}\}^{\mathrm{T}}$ and $\dot{\boldsymbol{v}}_{\mathrm{S}i} = \{\ddot{\mathrm{x}}_{\mathrm{S}i}\ \ddot{\mathrm{y}}_{\mathrm{S}i}\ \ddot{\mathrm{z}}_{\mathrm{S}i}\}^{\mathrm{T}}$ are the acceleration vector of the MP and acceleration vector of ith S-joint, respectively. Matrix $\mathbf{N}_i$ and vector $\mathbf{m}_i$ can be found in "Appendix 1." Additionally, the acceleration of ith S-joint in $\{\mathcal{F}i\}$, ${}^{\mathcal{F}i}\dot{\boldsymbol{v}}_{\mathrm{S}i}$, can be written in terms of the velocities and accelerations of the actuators as follows

$$\begin{aligned}{}^{\mathcal{F}i}\dot{\boldsymbol{v}}_{\mathrm{S}i} &= {}^{\mathcal{F}i}_{\mathrm{B}}\mathbf{R}\dot{\boldsymbol{v}}_{\mathrm{S}i} = \ddot{\mathrm{q}}^{\mathrm{ac}}_i{}^{\mathcal{F}i}\hat{\mathbf{q}}^{\mathrm{ac}}_i + 2\dot{\mathrm{q}}^{\mathrm{ac}}_i{}^{\mathcal{F}i}\boldsymbol{\omega}_{\mathrm{Leg},i}\\ &\quad \times {}^{\mathcal{F}i}\hat{\mathbf{q}}^{\mathrm{ac}}_i{}^{\mathcal{F}i}\dot{\boldsymbol{\omega}}_{\mathrm{Leg},i}\times{}^{\mathcal{F}i}\hat{\mathbf{q}}^{\mathrm{ac}}_i\\ &\quad + \mathrm{q}^{\mathrm{ac}}_i{}^{\mathcal{F}i}\boldsymbol{\omega}_{\mathrm{Leg},i}\times\left({}^{\mathcal{F}i}\boldsymbol{\omega}_{\mathrm{Leg},i}\times{}^{\mathcal{F}i}\hat{\mathbf{q}}^{\mathrm{ac}}_i\right)\\ &\quad \text{for} \quad i=1,\ldots,6\end{aligned} \tag{39}$$

By dot multiplying two sides of Eq. (39) with ${}^{\mathcal{F}i}\hat{\mathbf{q}}^{\mathrm{ac}}_i$, the inverse acceleration relation is obtained as

$$\begin{aligned}\ddot{\mathrm{q}}^{\mathrm{ac}}_i &= {}^{\mathcal{F}i}\boldsymbol{v}_{\mathrm{S}i}\,.\,{}^{\mathcal{F}i}\hat{\mathbf{q}}^{\mathrm{ac}}_i - q^{\mathrm{ac}}_i\Omega_i = {}^{\mathcal{F}i}\ddot{\mathrm{z}}_{\mathrm{S}i} - q^{\mathrm{ac}}_i\Omega_i\\ &\quad \text{for} \quad i=1,\ldots,6\end{aligned} \tag{40}$$

where ${}^{\mathcal{F}i}\dot{\boldsymbol{v}}_{\mathrm{S}i}\,.\,{}^{\mathcal{F}i}\hat{\mathbf{q}}^{\mathrm{ac}}_i = {}^{\mathcal{F}i}\ddot{\mathrm{z}}_{\mathrm{S}i}$ and

$$\begin{aligned}\Omega_i &= \left\{{}^{\mathcal{F}i}\boldsymbol{\omega}_{\mathrm{Leg},i}\times\left({}^{\mathcal{F}i}\boldsymbol{\omega}_{\mathrm{Leg},i}\times{}^{\mathcal{F}i}\hat{\mathbf{q}}^{\mathrm{ac}}_i\right)\right\}.{}^{\mathcal{F}i}\hat{\mathbf{q}}^{\mathrm{ac}}_i\\ &= -\left({}^{\mathcal{F}i}\omega^2_{\mathrm{Leg},ix} + {}^{\mathcal{F}i}\omega^2_{\mathrm{Leg},iy}\right)\\ &\quad \text{for} \quad i=1,\ldots,6\end{aligned} \tag{41}$$

Therefore, value of Ω_i can be obtained using Eqs. (28) or (33) as function of $\mathbf{t}_{\mathrm{MP}}$ or $\dot{\mathbf{q}}^{\mathrm{ac}}$, respectively. Also, to obtain value of ${}^{\mathcal{F}i}\ddot{\mathrm{z}}_{\mathrm{S}i}$, Eq. (38) is employed as follows

$$^{\mathcal{F}i}\dot{\boldsymbol{\nu}}_{Si} = {}^{\mathcal{F}i}_{\mathrm{B}}\mathbf{R}\dot{\boldsymbol{\nu}}_{Si} = {}^{\mathcal{F}i}\mathbf{J}_{\mathrm{MP}i}\dot{\mathbf{t}}_{\mathrm{MP}} + {}^{\mathcal{F}i}\mathbf{N}_i\boldsymbol{\omega}_{\mathrm{MP}} + {}^{\mathcal{F}i}\mathbf{m}_i \quad \text{for} \quad i = 1, \ldots, 6 \tag{42}$$

where $^{\mathcal{F}i}\mathbf{N}_i = {}^{\mathcal{F}i}_{\mathrm{B}}\mathbf{R}\mathbf{N}_i$ and $^{\mathcal{F}i}\mathbf{m}_i = {}^{\mathcal{F}i}_{\mathrm{B}}\mathbf{R}\mathbf{m}_i$. Substituting Eqs. (41)–(42) into (40) and rewriting Eq. (40) in a familiar matrix form, we have

$$\ddot{\mathbf{q}}^{\mathrm{ac}} = \mathbf{J}_{\mathrm{MP}}\dot{\mathbf{t}}_{\mathrm{MP}} + \mathbf{N}\boldsymbol{\omega}_{\mathrm{MP}} + \mathbf{m} \tag{43}$$

Equation (43) is called the *overall inverse acceleration* relation of the 6-UPS parallel robot where $\ddot{\mathbf{q}}^{\mathrm{ac}} = \{\ddot{\mathrm{q}}_1^{\mathrm{ac}}, \ldots, \ddot{\mathrm{q}}_6^{\mathrm{ac}}\}^{\mathrm{T}}$ is vector of the linear actuated joint accelerations and $\mathbf{N}$ is a 6×3 matrix as well as $\mathbf{m}$ is a 6×1 vector which are shown in "Appendix 1." Note that, the angular acceleration of the MP, $\dot{\boldsymbol{\omega}}_{\mathrm{MP}}$, can be obtained by time differentiating from Eqs. (107) or (108). For more explanations, see "Appendix 4." Furthermore, the overall direct acceleration relation of the robot can be obtained using Eq. (43) as follows

$$\dot{\mathbf{t}}_{\mathrm{MP}} = \mathbf{J}_{\mathrm{MP}}^{-1}\ddot{\mathbf{q}}^{\mathrm{ac}} - \mathbf{J}_{\mathrm{MP}}^{-1}(\mathbf{N}\boldsymbol{\omega}_{\mathrm{MP}} + \mathbf{m}) \tag{44}$$

To obtain the overall direct acceleration relation as a function of $\ddot{\mathbf{q}}^{\mathrm{ac}}$ and $\dot{\mathbf{q}}^{\mathrm{ac}}$, vectors $\boldsymbol{\omega}_{\mathrm{MP}}$ and $\mathbf{m}$ must be obtained as functions of $\dot{\mathbf{q}}^{\mathrm{ac}}$. Therefore, Eq. (44) can be rewritten as

$$\dot{\mathbf{t}}_{\mathrm{MP}} = \mathbf{J}_{\mathrm{MP}}^{-1}\ddot{\mathbf{q}}^{\mathrm{ac}} + \mathbf{J}_{\mathrm{Cor,MP}}\dot{\mathbf{q}}^{\mathrm{ac}} \tag{45}$$

"Appendix 2" provides the derivation of matrix $\mathbf{J}_{\mathrm{Cor,MP}}$.

6 Link acceleration analysis

As stated earlier, since two rotation axes of the ith robot's leg, $\hat{\mathbf{e}}_{\gamma i}$ and $\hat{\mathbf{e}}_{\psi i}$, are not always perpendicular to the leg, we cannot state that the ith leg of 6-UPS robot does not have spin about z-axis of frame $\{\mathcal{F}_i\}$ (see Fig. 2a). In other words, $\dot{\boldsymbol{\omega}}_{\mathrm{Leg},i} \cdot \hat{\mathbf{q}}_i^{\mathrm{ac}}$ is not always equal to zero. Therefore, the angular acceleration of ith leg in its local frame $\{\mathcal{F}_i\}$, $^{\mathcal{F}i}\dot{\boldsymbol{\omega}}_{\mathrm{Leg},i}$ cannot be always obtained using cross product of both sides of Eq. (39) with unit vector $^{\mathcal{F}i}\hat{\mathbf{q}}_i^{\mathrm{ac}}$. Similar to the previous derivation to obtain the link velocity relations, the angular acceleration of ith leg can be obtained using the direct time differentiation of Eqs. (20) or (22). This yield

$$^{\mathcal{F}i}\dot{\boldsymbol{\omega}}_{\mathrm{Leg},i} = \ddot{\gamma}_i\,{}^{\mathcal{F}i}\hat{\mathbf{e}}_{\gamma i} + \ddot{\psi}_i\,{}^{\mathcal{F}i}\hat{\mathbf{e}}_{\psi i} + \dot{\psi}_i\left(\dot{\gamma}_i\,{}^{\mathcal{F}i}\hat{\mathbf{e}}_{\gamma i} \times {}^{\mathcal{F}i}\hat{\mathbf{e}}_{\psi i}\right) \quad \text{for } i = 1, \ldots, 6 \tag{46}$$

Note that the direction of $^{\mathcal{F}i}\hat{\mathbf{e}}_{\gamma i}$ remains unchanged. Therefore, we can write

$$\begin{aligned} {}^{\mathcal{F}i}\dot{\boldsymbol{\omega}}_{\mathrm{Leg},i} &= {}^{\mathcal{F}i}\dot{\mathbf{k}}_{\mathrm{U}i}\begin{Bmatrix}\dot{\gamma}_i\\ \dot{\psi}_i\end{Bmatrix} + {}^{\mathcal{F}i}\mathbf{k}_{\mathrm{U}i}\begin{Bmatrix}\ddot{\gamma}_i\\ \ddot{\psi}_i\end{Bmatrix} \\ &= \begin{Bmatrix}\ddot{\psi}_i\\ \ddot{\gamma}_i\cos(\psi_i) - \dot{\psi}_i\dot{\gamma}_i\sin(\psi_i)\\ -\ddot{\gamma}_i\sin(\psi_i) - \dot{\psi}_i\dot{\gamma}_i\cos(\psi_i)\end{Bmatrix} \\ &\quad \text{for} \quad i = 1, \ldots, 6 \end{aligned} \tag{47}$$

where $^{\mathcal{F}i}\dot{\mathbf{k}}_{\mathrm{U}i} = \mathrm{d}(^{\mathcal{F}i}\mathbf{k}_{\mathrm{U}i})/\mathrm{d}t$. The values of $\dot{\gamma}_i$ and $\dot{\psi}_i$ are obtained in Eq. (27). The cross product of both sides of Eq. (39) with unit vector $^{\mathcal{F}i}\hat{\mathbf{q}}_i^{\mathrm{ac}}$ leads to obtain values of $\ddot{\gamma}_i$ and $\ddot{\psi}_i$. "Appendix 3" represents the derivation of $\ddot{\gamma}_i$ and $\ddot{\psi}_i$. Therefore, the angular acceleration of ith leg, $^{\mathcal{F}i}\dot{\boldsymbol{\omega}}_{\mathrm{Leg},i}$ will be rewritten in terms of the end-effector acceleration vector in compact form as follows

$$^{\mathcal{F}i}\dot{\boldsymbol{\omega}}_{\mathrm{Leg},i} = \mathbf{J}_{\omega i}\dot{\mathbf{t}}_{\mathrm{MP}} + \boldsymbol{\Omega}_{\omega i}\mathbf{t}_{\mathrm{MP}} + \mathbf{N}_{\omega i}\boldsymbol{\omega}_{\mathrm{MP}} + \mathbf{m}_{\omega i} \quad \text{for} \quad i = 1, \ldots, 6 \tag{48}$$

The 3×6 Matrix $\boldsymbol{\Omega}_{\omega i}$ and 3×3 matrix $\mathbf{N}_{\omega i}$ as well as vector $\mathbf{m}_{\omega i}$ are found in "Appendix 1." The mass centers' accelerations of the actuators' cylinder and piston can be derived by time differentiating from Eq. (29). These yields

$$\begin{aligned} {}^{\mathcal{F}i}\dot{\boldsymbol{\nu}}_{\mathrm{C.G.1}\,i} &= \mathrm{e}_1\,{}^{\mathcal{F}i}\dot{\boldsymbol{\omega}}_{\mathrm{Leg},i} \times {}^{\mathcal{F}i}\hat{\mathbf{q}}_i^{\mathrm{ac}} + \mathrm{e}_1\,{}^{\mathcal{F}i}\boldsymbol{\omega}_{\mathrm{Leg},i} \\ &\quad \times \left({}^{\mathcal{F}i}\boldsymbol{\omega}_{\mathrm{Leg},i} \times {}^{\mathcal{F}i}\hat{\mathbf{q}}_i^{\mathrm{ac}}\right) \\ {}^{\mathcal{F}i}\dot{\boldsymbol{\nu}}_{\mathrm{C.G.2}\,i} &= \ddot{\mathrm{q}}_i^{\mathrm{ac}}\,{}^{\mathcal{F}i}\hat{\mathbf{q}}_i^{\mathrm{ac}} + 2\dot{\mathrm{q}}_i^{\mathrm{ac}}\,{}^{\mathcal{F}i}\boldsymbol{\omega}_{\mathrm{Leg},i} \\ &\quad \times {}^{\mathcal{F}i}\hat{\mathbf{q}}_i^{\mathrm{ac}} + \left(\mathrm{q}_i^{\mathrm{ac}} - \mathrm{e}_2\right){}^{\mathcal{F}i}\dot{\boldsymbol{\omega}}_{\mathrm{Leg},i} \\ &\quad \times {}^{\mathcal{F}i}\hat{\mathbf{q}}_i^{\mathrm{ac}} + \left(\mathrm{q}_i^{\mathrm{ac}} - \mathrm{e}_2\right){}^{\mathcal{F}i}\boldsymbol{\omega}_{\mathrm{Leg},i} \\ &\quad \times \left({}^{\mathcal{F}i}\boldsymbol{\omega}_{\mathrm{Leg},i} \times {}^{\mathcal{F}i}\hat{\mathbf{q}}_i^{\mathrm{ac}}\right) \\ &\quad \text{for} \quad i = 1, \ldots, 6 \end{aligned} \tag{49}$$

Therefore, Eq. (49) can be rewritten in terms of the end-effector acceleration vector in compact form using Eqs. (17), (28), (43) and (48) as follows

$$\begin{aligned} {}^{\mathcal{F}i}\dot{\boldsymbol{\nu}}_{\mathrm{C.G.1}\,i} &= \mathbf{J}_{v1,i}\dot{\mathbf{t}}_{\mathrm{MP}} + \boldsymbol{\Omega}_{v1,i}\mathbf{t}_{\mathrm{MP}} \\ &\quad + \mathbf{N}_{v1,i}\boldsymbol{\omega}_{\mathrm{MP}} + \mathbf{m}_{v1,i} \\ {}^{\mathcal{F}i}\dot{\boldsymbol{\nu}}_{\mathrm{C.G.2}\,i} &= \mathbf{J}_{v2,i}\dot{\mathbf{t}}_{\mathrm{MP}} + \boldsymbol{\Omega}_{v2,i}\mathbf{t}_{\mathrm{MP}} \\ &\quad + \mathbf{N}_{v2,i}\boldsymbol{\omega}_{\mathrm{MP}} + \mathbf{m}_{v2,i} \\ &\quad \text{for} \quad i = 1, \ldots, 6 \end{aligned} \tag{50}$$

The matrices $\boldsymbol{\Omega}_{v1,i}$, $\boldsymbol{\Omega}_{v2,i}$, $\mathbf{N}_{v1,i}$ and $\mathbf{N}_{v2,i}$ as well as vectors $\mathbf{m}_{v1,i}$ and $\mathbf{m}_{v2,i}$ are presented in "Appendix 1." Equations (48) and (50) are called the *inverse*

link acceleration relations. By combining these equations, the *overall inverse link acceleration relations* are obtained as

$$\begin{aligned}
{}^{\mathcal{F}i}\dot{\mathbf{t}}_{\mathrm{cyl},i} &= \mathbf{J}_{\mathrm{inv,cyl},i}\dot{\mathbf{t}}_{\mathrm{MP}} + \boldsymbol{\Omega}_{\mathrm{inv,cyl},i}\mathbf{t}_{\mathrm{MP}} \\
&\quad + \mathbf{N}_{\mathrm{inv,cyl},i}\boldsymbol{\omega}_{\mathrm{MP}} + \mathbf{m}_{\mathrm{inv,cyl},i} \\
{}^{\mathcal{F}i}\dot{\mathbf{t}}_{\mathrm{pis},i} &= \mathbf{J}_{\mathrm{inv,pis},i}\dot{\mathbf{t}}_{\mathrm{MP}} + \boldsymbol{\Omega}_{\mathrm{inv,pis},i}\mathbf{t}_{\mathrm{MP}} \\
&\quad + \mathbf{N}_{\mathrm{inv,pis},i}\boldsymbol{\omega}_{\mathrm{MP}} + \mathbf{m}_{\mathrm{inv,pis},i} \\
&\quad \text{for} \quad i = 1, \ldots, 6
\end{aligned} \tag{51}$$

where

$$\begin{aligned}
\mathbf{J}_{\mathrm{inv,cyl},i} &= \begin{bmatrix} \mathbf{J}_{v1,i} \\ \mathbf{J}_{\omega i} \end{bmatrix}, \quad \boldsymbol{\Omega}_{\mathrm{inv,cyl},i} = \begin{bmatrix} \boldsymbol{\Omega}_{v1,i} \\ \boldsymbol{\Omega}_{\omega i} \end{bmatrix}, \\
\mathbf{N}_{\mathrm{inv,cyl},i} &= \begin{bmatrix} \mathbf{N}_{v1,i} \\ \mathbf{N}_{\omega i} \end{bmatrix}, \quad \mathbf{m}_{\mathrm{inv,cyl},i} = \begin{bmatrix} \mathbf{m}_{v1,i} \\ \mathbf{m}_{\omega i} \end{bmatrix} \\
\mathbf{J}_{\mathrm{inv,pis},i} &= \begin{bmatrix} \mathbf{J}_{v2,i} \\ \mathbf{J}_{\omega i} \end{bmatrix}, \quad \boldsymbol{\Omega}_{\mathrm{inv,pis},i} = \begin{bmatrix} \boldsymbol{\Omega}_{v2,i} \\ \boldsymbol{\Omega}_{\omega i} \end{bmatrix}, \\
\mathbf{N}_{\mathrm{inv,pis},i} &= \begin{bmatrix} \mathbf{N}_{v2,i} \\ \mathbf{N}_{\omega i} \end{bmatrix}, \quad \mathbf{m}_{\mathrm{inv,pis},i} = \begin{bmatrix} \mathbf{m}_{v2,i} \\ \mathbf{m}_{\omega i} \end{bmatrix} \\
&\quad \text{for} \quad i = 1, \ldots, 6
\end{aligned} \tag{52}$$

Note that, ${}^{\mathcal{F}i}\dot{\mathbf{t}}_{\mathrm{cyl},i} = \{{}^{\mathcal{F}i}\dot{\boldsymbol{\nu}}^{\mathrm{T}}_{\mathrm{C.G.1}\ i} \quad {}^{\mathcal{F}i}\dot{\boldsymbol{\omega}}^{\mathrm{T}}_{\mathrm{Leg},i}\}^{\mathrm{T}}$ and ${}^{\mathcal{F}i}\dot{\mathbf{t}}_{\mathrm{pis},i} = \{{}^{\mathcal{F}i}\dot{\boldsymbol{\nu}}^{\mathrm{T}}_{\mathrm{C.G.2}\ i} \quad {}^{\mathcal{F}i}\dot{\boldsymbol{\omega}}^{\mathrm{T}}_{\mathrm{Leg},i}\}^{\mathrm{T}}$ represent the acceleration vectors of cylinder and piston of the ith robot's leg, respectively. Furthermore, obtaining the overall acceleration vectors of each leg in terms of $\ddot{\mathbf{q}}^{\mathrm{ac}}$ and $\ddot{\mathbf{q}}^{\mathrm{ac}}$ is necessary to derive the direct dynamics relations. To do this, first, substitute vectors $\boldsymbol{\omega}_{\mathrm{MP}}$ and $\mathbf{t}_{\mathrm{MP}}$ from Eq. (18) and vector $\dot{\mathbf{t}}_{\mathrm{MP}}$ from Eqs. (45) into (51). Then vectors $\mathbf{m}_{\omega_i}$, $\mathbf{m}_{v1,i}$ and $\mathbf{m}_{v2,i}$ should be obtained as function of $\dot{\mathbf{q}}^{\mathrm{ac}}$. This procedure is presented in "Appendix 3." Therefore, the *overall direct link acceleration relations* can be derived as follows

$$\begin{aligned}
{}^{\mathcal{F}i}\dot{\mathbf{t}}_{\mathrm{cyl},i} &= \mathbf{J}_{\mathrm{dir,cyl},i}\ddot{\mathbf{q}}^{\mathrm{ac}} + \mathbf{J}_{\mathrm{Col,cyl},i}\dot{\mathbf{q}}^{\mathrm{ac}} \\
{}^{\mathcal{F}i}\dot{\mathbf{t}}_{\mathrm{cyl},i} &= \mathbf{J}_{\mathrm{dir,cyl},i}\ddot{\mathbf{q}}^{\mathrm{ac}} + \mathbf{J}_{\mathrm{Col,cyl},i}\dot{\mathbf{q}}^{\mathrm{ac}} \\
&\quad \text{for} \quad i = 1, \ldots, 6
\end{aligned} \tag{53}$$

where $\mathbf{J}_{\mathrm{dir,cyl},i}$ and $\mathbf{J}_{\mathrm{dir,pis},i}$ are obtained in Eq. (34). Also, "Appendix 3" represents the derivation of $\mathbf{J}_{\mathrm{Cor,cyl},i}$ and $\mathbf{J}_{\mathrm{Cor,pis},i}$.

7 Rigid body dynamics

The direct dynamics problem aims to find the response of a robot arm corresponding to given applied actuators' moments or forces. That is, given the vector of actuated joint moments/forces, it computes the resulting motion of the manipulator as a function of time. In the present paper, the principle of virtual work is utilized to compute the actuated forces.

To obtain the equations of motion, the resultant force/torque due to all rigid bodies can be considered. In this subsection, we obtain the resultant wrench due to applied external wrench for the MP and limbs as function of position, $\mathbf{q}^{\mathrm{ac}}$, velocity, $\dot{\mathbf{q}}^{\mathrm{ac}}$, and acceleration, $\ddot{\mathbf{q}}^{\mathrm{ac}}$, of the prismatic actuators. In the direct dynamics problem, the vector of initial actuated joint positions, vector of initial actuated joint velocities and applied actuator forces are given and the resultant position, velocity and acceleration of the MP are obtained.

7.1 Resultant wrench due to applied external wrench and inertia of the MP

The resultant wrench due to applied external wrench and inertia of the MP in the base frame {B}, $\mathbf{w}_{\mathrm{MP}}$ can be written as

$$\begin{aligned}
\mathbf{w}_{\mathrm{MP}} &= \begin{Bmatrix} \mathbf{f}_{\mathrm{MP}} \\ \mathbf{n}_{\mathrm{MP}} \end{Bmatrix} = \begin{Bmatrix} \mathbf{f}_{\mathrm{ext}} \\ \mathbf{n}_{\mathrm{ext}} \end{Bmatrix} + \begin{Bmatrix} \mathrm{m}_{\mathrm{MP}}\mathbf{g} \\ \mathbf{0}_{3\times 1} \end{Bmatrix} \\
&\quad + \begin{Bmatrix} -\mathrm{m}_{\mathrm{MP}}\dot{\boldsymbol{\nu}}_{\mathrm{p}} \\ -{}^{\mathrm{B}}\mathbf{I}_{\mathrm{MP}}\ \dot{\boldsymbol{\omega}}_{\mathrm{MP}} - \boldsymbol{\omega}_{\mathrm{MP}} \times \left({}^{\mathrm{B}}\mathbf{I}_{\mathrm{MP}}\ \boldsymbol{\omega}_{\mathrm{MP}}\right) \end{Bmatrix}
\end{aligned} \tag{54}$$

where m_{MP} and ${}^{\mathrm{B}}\mathbf{I}_{\mathrm{MP}}$ are the mass and inertia matrix of the MP, respectively. Vectors $\mathbf{f}_{\mathrm{ext}}$ and $\mathbf{n}_{\mathrm{ext}}$ are applied external force and moment exerted to end-effector which are all defined in frame {B} as

$$\begin{aligned}
&\mathbf{f}_{\mathrm{ext}} = \begin{Bmatrix} f_x & f_y & f_z \end{Bmatrix}^{\mathrm{T}}, \quad \mathbf{n}_{\mathrm{ext}} = \begin{Bmatrix} n_x & n_y & n_z \end{Bmatrix}^{\mathrm{T}}, \\
&{}^{\mathrm{B}}\mathbf{I}_{\mathrm{MP}} = {}^{\mathrm{B}}_{\mathrm{T}}\mathbf{R}\ {}^{\mathrm{T}}\mathbf{I}_{\mathrm{MP}}\ {}^{\mathrm{T}}_{\mathrm{B}}\mathbf{R}
\end{aligned} \tag{55}$$

Also, vector $\mathbf{g}$ is the gravitational acceleration vector which is defined in frame {B} as

$$\mathbf{g} = \begin{Bmatrix} g_x = 0 & g_y = 0 & g_z = 9.81 \end{Bmatrix}^{\mathrm{T}} \tag{56}$$

We can state that

$$\begin{aligned}
&\boldsymbol{\omega}_{\mathrm{MP}} \times \left({}^{\mathrm{B}}\mathbf{I}_{\mathrm{MP}}\ \boldsymbol{\omega}_{\mathrm{MP}}\right) = (\boldsymbol{\omega}_{\mathrm{MP}} \times \mathbf{I}_{3\times 3})\,{}^{\mathrm{B}}\mathbf{I}_{\mathrm{MP}}\ \boldsymbol{\omega}_{\mathrm{MP}} \\
&= (\boldsymbol{\omega}_{\mathrm{MP}} \times \mathbf{I}_{3\times 3})\,{}^{\mathrm{B}}\mathbf{I}_{\mathrm{MP}}\ \mathbf{J}^{-1}_{\mathrm{MP}(4-6)\times 6}\dot{\mathbf{q}}^{\mathrm{ac}}
\end{aligned} \tag{57}$$

By substituting $\boldsymbol{\omega}_{\mathrm{MP}}$, $\dot{\boldsymbol{\nu}}_{\mathrm{p}}$ and $\dot{\boldsymbol{\omega}}_{\mathrm{MP}}$ from Eqs. (18) and (45) into Eq. (54), vector $\mathbf{w}_{\mathrm{MP}}$ can be obtained in terms of $\dot{\mathbf{q}}^{\mathrm{ac}}$ and $\ddot{\mathbf{q}}^{\mathrm{ac}}$ as follows

$$\mathbf{w}_{\mathrm{MP}} = \mathbf{M}_{\mathrm{MP}}(\mathbf{q})\ddot{\mathbf{q}}^{\mathrm{ac}} + \mathbf{C}_{\mathrm{MP}}(\mathbf{q},\dot{\mathbf{q}})\dot{\mathbf{q}}^{\mathrm{ac}} + \mathbf{w}_{g_{\mathrm{MP}}} + \mathbf{w}_{\mathrm{ext}} \tag{58}$$

where matrices $\mathbf{M}_{\mathrm{MP}}$ and $\mathbf{C}_{\mathrm{MP}}$ as well as vectors $\mathbf{w}_{g_{\mathrm{MP}}}$ and $\mathbf{w}_{\mathrm{ext}}$ are shown in "Appendix 1."

7.2 Resultant wrench due to inertia of the cylinder and piston of actuators

The resultant wrench due to inertia of the cylinder and piston of ith actuators in its local frame $\{\mathcal{F}_i\}$, ${}^{\mathcal{F}i}\mathbf{w}_{\mathrm{Leg},i}$, can be written as follows

$$\begin{aligned}
{}^{\mathcal{F}i}\mathbf{w}_{\mathrm{cyl},i} &= \begin{Bmatrix} \mathbf{f}_{\mathrm{cyl},i} \\ \mathbf{n}_{\mathrm{cyl},i} \end{Bmatrix} = \begin{Bmatrix} \mathrm{m}_{\mathrm{cyl},i}\,{}^{\mathcal{F}i}_{\mathrm{B}}\mathbf{R}\mathbf{g} \\ \mathbf{0}_{3\times 1} \end{Bmatrix} \\
&+ \begin{Bmatrix} -\mathrm{m}_{\mathrm{cyl},i}\,{}^{\mathcal{F}i}\dot{\boldsymbol{v}}_{\mathrm{C.G.1}i} \\ -{}^{\mathcal{F}i}\mathbf{I}_{\mathrm{cyl},i}\,{}^{\mathcal{F}i}\dot{\boldsymbol{\omega}}_{\mathrm{Leg},i} - {}^{\mathcal{F}i}\dot{\boldsymbol{\omega}}_{\mathrm{Leg},i} \times \left({}^{\mathcal{F}i}\mathbf{I}_{\mathrm{cyl},i}\ {}^{\mathcal{F}i}\boldsymbol{\omega}_{\mathrm{Leg},i}\right) \end{Bmatrix} \\
{}^{\mathcal{F}i}\mathbf{w}_{\mathrm{pis},i} &= \begin{Bmatrix} \mathbf{f}_{\mathrm{pis},i} \\ \mathbf{n}_{\mathrm{pis},i} \end{Bmatrix} = \begin{Bmatrix} \mathrm{m}_{\mathrm{pis},i}\,{}^{\mathcal{F}i}_{\mathrm{B}}\mathbf{R}\mathbf{g} \\ \mathbf{0}_{3\times 1} \end{Bmatrix} \\
&+ \begin{Bmatrix} -\mathrm{m}_{\mathrm{pis},i}\,{}^{\mathcal{F}i}\dot{\boldsymbol{v}}_{\mathrm{C.G.1}i} \\ -{}^{\mathcal{F}i}\mathbf{I}_{\mathrm{pis},i}\,{}^{\mathcal{F}i}\dot{\boldsymbol{\omega}}_{\mathrm{Leg},i} - {}^{\mathcal{F}i}\dot{\boldsymbol{\omega}}_{\mathrm{Leg},i} \times \left({}^{\mathcal{F}i}\mathbf{I}_{\mathrm{pis},i}\ {}^{\mathcal{F}i}\boldsymbol{\omega}_{\mathrm{Leg},i}\right) \end{Bmatrix} \\
&\text{for} \quad i = 1,\ldots,6
\end{aligned} \tag{59}$$

where $m_{\mathrm{cyl},i}$ and $m_{\mathrm{pis},i}$ are the mass of the cylinder and piston of the ith leg. We can state

$$\begin{aligned}
&{}^{\mathcal{F}i}\boldsymbol{\omega}_{\mathrm{Leg},i} \times \left({}^{\mathcal{F}i}\mathbf{I}_{\mathrm{cyl},i}\,{}^{\mathcal{F}i}\boldsymbol{\omega}_{\mathrm{Leg},i}\right) \\
&= \left({}^{\mathcal{F}i}\boldsymbol{\omega}_{\mathrm{Leg},i} \times \mathbf{I}_{3\times 3}\right){}^{\mathcal{F}i}\mathbf{I}_{\mathrm{cyl},i}\ \mathbf{J}_{\omega i}\ \mathbf{J}_{\mathrm{MP}}^{-1}\,\dot{\mathbf{q}}^{\mathrm{ac}} \\
&{}^{\mathcal{F}i}\boldsymbol{\omega}_{\mathrm{Leg},i} \times \left({}^{\mathcal{F}i}\mathbf{I}_{\mathrm{pis},i}\,{}^{\mathcal{F}i}\boldsymbol{\omega}_{\mathrm{Leg},i}\right) \\
&= \left({}^{\mathcal{F}i}\boldsymbol{\omega}_{\mathrm{Leg},i} \times \mathbf{I}_{3\times 3}\right){}^{\mathcal{F}i}\mathbf{I}_{\mathrm{pis},i}\ \mathbf{J}_{\omega i}\ \mathbf{J}_{\mathrm{MP}}^{-1}\,\dot{\mathbf{q}}^{\mathrm{ac}} \\
&\text{for} \quad i = 1,\ldots,6
\end{aligned} \tag{60}$$

By substituting ${}^{\mathcal{F}i}\boldsymbol{\omega}_{\mathrm{Leg},i}$, ${}^{\mathcal{F}i}\dot{\boldsymbol{\omega}}_{\mathrm{Leg},i}$, ${}^{\mathcal{F}i}\dot{\boldsymbol{v}}_{\mathrm{C.G.1},i}$ and ${}^{\mathcal{F}i}\dot{\boldsymbol{v}}_{\mathrm{C.G.2},i}$ from Eqs. (34) and (51) into Eq. (59), vectors ${}^{\mathcal{F}i}\mathbf{w}_{\mathrm{cyl},i}$ and ${}^{\mathcal{F}i}\mathbf{w}_{\mathrm{pis},i}$ can be obtained in terms of $\dot{\mathbf{q}}^{\mathrm{ac}}$ and $\ddot{\mathbf{q}}^{\mathrm{ac}}$ as follows

$$\begin{aligned}
{}^{\mathcal{F}i}\mathbf{w}_{\mathrm{cyl},i} &= \mathbf{M}_{\mathrm{cyl},i}(\mathbf{q})\,\ddot{\mathbf{q}}^{\mathrm{ac}} + \mathbf{C}_{\mathrm{cyl},i}(\mathbf{q},\dot{\mathbf{q}})\dot{\mathbf{q}}^{\mathrm{ac}} + \mathbf{w}_{g_{\mathrm{cyl},i}} \\
{}^{\mathcal{F}i}\mathbf{w}_{\mathrm{pis},i} &= \mathbf{M}_{\mathrm{pis},i}(\mathbf{q})\,\ddot{\mathbf{q}}^{\mathrm{ac}} + \mathbf{C}_{\mathrm{pis},i}(\mathbf{q},\dot{\mathbf{q}})\dot{\mathbf{q}}^{\mathrm{ac}} + \mathbf{w}_{g_{\mathrm{pis},i}} \\
&\text{for} \quad i = 1,\ldots,6
\end{aligned} \tag{61}$$

where matrices $\mathbf{M}_{\mathrm{cyl},i}$, $\mathbf{M}_{\mathrm{pis},i}$, $\mathbf{C}_{\mathrm{cyl},i}$ and $\mathbf{C}_{\mathrm{pis},i}$ as well as vectors $\mathbf{w}_{g_{\mathrm{cyl},i}}$ and $\mathbf{w}_{g_{\mathrm{pis},i}}$ are shown in "Appendix 1."

7.3 Equations of motion

Using principle of virtual work, the equations of motion of the robot can be expressed as

$$\begin{aligned}
&\left(\delta\mathbf{q}^{\mathrm{ac}}\right)^{\mathrm{T}}\mathbf{f}^{\mathrm{ac}} + \left(\delta\mathbf{t}_{\mathrm{MP}}\right)^{\mathrm{T}}\mathbf{w}_{\mathrm{MP}} \\
&+ \sum_{i=1}^{6}\left(\left(\delta^{\mathcal{F}i}\mathbf{t}_{\mathrm{cyl},i}\right)^{\mathrm{T}}{}^{\mathcal{F}i}\mathbf{w}_{\mathrm{cyl},i}\right. \\
&\left. + \left(\delta^{\mathcal{F}i}\mathbf{t}_{\mathrm{pis},i}\right)^{\mathrm{T}}{}^{\mathcal{F}i}\mathbf{w}_{\mathrm{pis},i}\right) = \mathbf{0}
\end{aligned} \tag{62}$$

where $\delta\mathbf{q}^{\mathrm{ac}}$ is the virtual translational vector of the actuated joints and $\delta\mathbf{t}_{\mathrm{MP}}$ is the virtual twist vector of the MP. Vector $\mathbf{f}^{\mathrm{ac}}$ is the actuated joints forces. Furthermore, $\delta^{\mathcal{F}i}\mathbf{t}_{\mathrm{cyl},i}$ and $\delta^{\mathcal{F}i}\mathbf{t}_{\mathrm{pis},i}$ are the virtual twist vector for cylinder and piston of the ith leg, respectively. The virtual twist vectors in Eq. (62) can be rewritten as functions of $\delta\mathbf{q}^{\mathrm{ac}}$. Consequently, using Eqs. (18) and (34), we have

$$\begin{aligned}
&\delta\mathbf{t}_{\mathrm{MP}} = \mathbf{J}_{\mathrm{MP}}^{-1}\delta\mathbf{q}^{\mathrm{ac}}, \\
&\delta^{\mathcal{F}i}\mathbf{t}_{\mathrm{cyl},i} = \mathbf{J}_{\mathrm{dir,cyl},i}\,\delta\mathbf{q}^{\mathrm{ac}}, \\
&\delta^{\mathcal{F}i}\mathbf{t}_{\mathrm{pis},i} = \mathbf{J}_{\mathrm{dir,pis},i}\,\delta\mathbf{q}^{\mathrm{ac}} \quad \text{for} \quad i = 1,\ldots,6
\end{aligned} \tag{63}$$

Substituting above equations as well as $\mathbf{w}_{\mathrm{MP}}$, ${}^{\mathcal{F}i}\mathbf{w}_{\mathrm{cyl},i}$ and ${}^{\mathcal{F}i}\mathbf{w}_{\mathrm{pis},i}$ from Eqs. (58) and (61) into Eq. (62) yield

$$\begin{aligned}
&\left(\delta\mathbf{q}^{\mathrm{ac}}\right)^{\mathrm{T}}\left(\mathbf{f}^{\mathrm{ac}} + \left(\mathbf{J}_{\mathrm{MP}}^{-\mathrm{T}}\mathbf{M}_{\mathrm{MP}} + \sum_{i=1}^{6}\left(\mathbf{J}_{\mathrm{dir,cyl},i}^{\mathrm{T}}\mathbf{M}_{\mathrm{cyl},i}\right.\right.\right. \\
&\left.\left.\left. + \mathbf{J}_{\mathrm{dir,pis},i}^{\mathrm{T}}\mathbf{M}_{\mathrm{pis},i}\right)\right)\ddot{\mathbf{q}}^{\mathrm{ac}} + \left(\mathbf{J}_{\mathrm{MP}}^{-\mathrm{T}}\mathbf{C}_{\mathrm{MP}}\right. \\
&\left. + \sum_{i=1}^{6}\left(\mathbf{J}_{\mathrm{dir,cyl},i}^{\mathrm{T}}\mathbf{C}_{\mathrm{cyl},i} + \mathbf{J}_{\mathrm{dir,pis},i}^{\mathrm{T}}\mathbf{C}_{\mathrm{pis},i}\right)\right)\dot{\mathbf{q}}^{\mathrm{ac}} \\
&+ \left(\mathbf{J}_{\mathrm{MP}}^{-\mathrm{T}}\mathbf{w}_{g_{\mathrm{MP}}} + \sum_{i=1}^{6}\left(\mathbf{J}_{\mathrm{dir,cyl},i}^{\mathrm{T}}\mathbf{w}_{g_{\mathrm{cyl},i}}\right.\right. \\
&\left.\left. + \mathbf{J}_{\mathrm{dir,pis},i}^{\mathrm{T}}\mathbf{w}_{g_{\mathrm{pis},i}}\right)\right) + \left(\mathbf{J}_{\mathrm{MP}}^{-\mathrm{T}}\mathbf{w}_{\mathrm{ext}}\right)\Big) = \mathbf{0}
\end{aligned} \tag{64}$$

Since Eq. (64) is valid for any $\delta\,\mathbf{q}^{\mathrm{ac}}$, it follows that

$$\mathbf{f}^{\mathrm{ac}} + \mathbf{M}(\mathbf{q})\,\ddot{\mathbf{q}}_{3\times 1}^{\mathrm{ac}} + \mathbf{C}(\mathbf{q},\dot{\mathbf{q}})\dot{\mathbf{q}}^{\mathrm{ac}} + \mathbf{G}(\mathbf{q}) + \mathbf{w} = \mathbf{0}_{6\times 1} \tag{65}$$

where

$$\begin{aligned}
\mathbf{M}(\mathbf{q}) &= \mathbf{J}_{\mathrm{MP}}^{-\mathrm{T}}\mathbf{M}_{\mathrm{MP}} \\
&\quad + \sum_{i=1}^{6}\left(\mathbf{J}_{\mathrm{dir,cyl},i}^{\mathrm{T}}\mathbf{M}_{\mathrm{cyl},i} + \mathbf{J}_{\mathrm{dir,pis},i}^{\mathrm{T}}\mathbf{M}_{\mathrm{pis},i}\right) \\
\mathbf{C}(\mathbf{q},\dot{\mathbf{q}}) &= \mathbf{J}_{\mathrm{MP}}^{-\mathrm{T}}\mathbf{C}_{\mathrm{MP}} \\
&\quad + \sum_{i=1}^{6}\left(\mathbf{J}_{\mathrm{dir,cyl},i}^{\mathrm{T}}\mathbf{C}_{\mathrm{cyl},i} + \mathbf{J}_{\mathrm{dir,pis},i}^{\mathrm{T}}\mathbf{C}_{\mathrm{pis},i}\right)
\end{aligned}$$

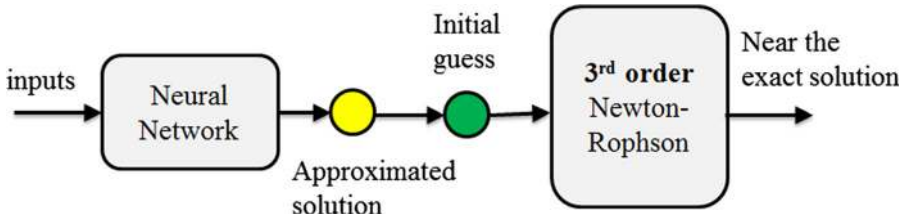

Fig. 3 The modified hybrid solution

$$\mathbf{G}(\mathbf{q}) = \mathbf{J}_{\mathrm{MP}}^{-\mathrm{T}}\mathbf{w}_{g_{\mathrm{MP}}} + \sum_{i=1}^{6}\left(\mathbf{J}_{\mathrm{dir,cyl},i}^{\mathrm{T}}\mathbf{w}_{g_{\mathrm{cyl},i}} + \mathbf{J}_{\mathrm{dir,pis},i}^{\mathrm{T}}\mathbf{w}_{g_{\mathrm{pis},i}}\right)$$
$$\mathbf{w} = \left(\mathbf{J}_{\mathrm{MP}}^{-\mathrm{T}}\mathbf{w}_{\mathrm{ext}}\right) \tag{66}$$

Most familiar Eq. (65) is the dynamics equation in terms of the actuators' velocity and acceleration vectors.

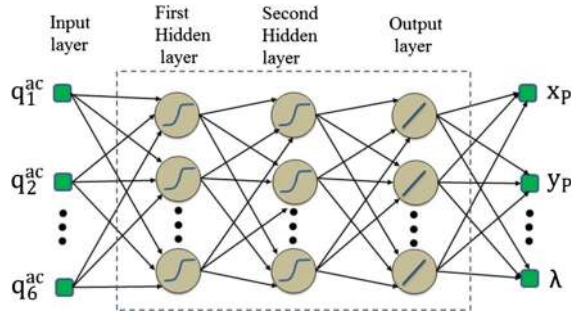

Fig. 4 MLPANN architecture for direct kinematics

8 Results and discussion

In this section, the paper's contributions are outlined and a discussion on improvements is presented. In direct kinematics, we are interested to determine the position and orientation of the mobile platform based on giving legs length. It should be mentioned that the direct kinematics of parallel robot, like Gough–Stewart platform, is very complicated than inverse kinematics. Therefore, we proposed a numerical method, like [30], to obtain a near-exact solution. In this paper, combination of neural network and third-order Newton–Raphson method is utilized to obtain modified hybrid strategies. This strategy is presented in Fig. 3. In this study, we used neural network, like [30], for initial guess and proposed using higher-order Newton–Raphson [31] to decrease the time of simulation.

For the modeling of DKP, the leg length of the 6-UPS robot as inputs and position and orientation of the MP as outputs of MLPANN are considered. Thus, here q_i^{ac} $(i = 1, \ldots, 6)$ as inputs and $\{x_{\mathrm{P}}, y_{\mathrm{P}}, z_{\mathrm{P}}, \theta, \varphi, \lambda\}$ as output of MLPANN is investigated.

To train the network, we need to suitable data that describe behavior of our models comprehensively. So, in this study the inverse kinematics is utilized to obtain these data. For this purpose, first the workspace of Gough–Stewart robot movement is specified. Then, by using inverse kinematics, the corresponding leg length of number of position and orientation in this workspace are obtained. Finally, the leg length and robot's Cartesian space parameters are used to input and outputs of MLPANN, respectively. This MLPANN is shown Fig. 4. Obviously, in this paper, two hidden layer were chosen for MLPANN. Also, we have chosen 15 nodes in the first layer and 20 nodes in the second layer.

As it mentioned before, we use MLPANN to fine the appropriate initial guess. If the initial guess is chosen near the acceptable solution, the Newton–Raphson method yields very accurate results, given a sufficient number of algorithm iterations [30,31]. For multiple equations and variables, Newton–Raphson's method is

$$\mathbf{X}_{m+1} = \mathbf{X}_m - \left(\frac{\partial \mathbf{F}(\mathbf{X}_m)}{\partial \mathbf{X}_m}\right)^{-1}\mathbf{F}(\mathbf{X}_m) \tag{67}$$

where $\mathbf{X}$ is a vector of the variables that we want to estimate, $\mathbf{F}$ is a vector function which approaches zero as the estimation of $\mathbf{X}$ and "m" represents iteration number.

For the robot considered in this study, we select

$$\mathbf{X}^{\mathrm{T}} = \{x_{\mathrm{P}}, y_{\mathrm{P}}, z_{\mathrm{P}}, \theta, \varphi, \lambda\} \tag{68}$$

and

$$\mathbf{F}(\mathbf{X}) = \begin{bmatrix} \left\|{}_{\mathrm{T}}^{\mathrm{B}}\mathbf{R}^{\mathrm{T}}\mathbf{b}_1 + \mathbf{p} - \mathbf{a}_1\right\| - l_1 \\ \vdots \\ \left\|{}_{\mathrm{T}}^{\mathrm{B}}\mathbf{R}^{\mathrm{T}}\mathbf{b}_2 + \mathbf{p} - \mathbf{a}_2\right\| - l_6 \end{bmatrix} = \begin{bmatrix} q_1^{\mathrm{ac}} - l_1 \\ \vdots \\ q_6^{\mathrm{ac}} - l_6 \end{bmatrix} \tag{69}$$

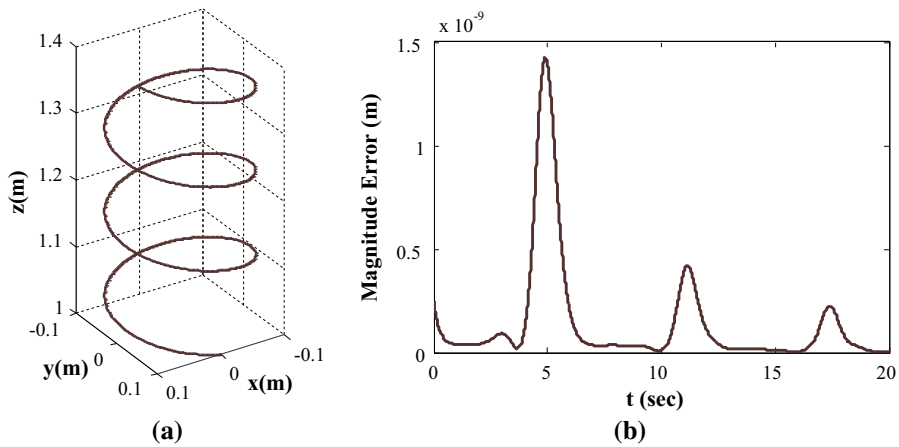

Fig. 5 **a** Desired trajectory and **b** error output of modified hybrid strategy

where q_i^{ac} and l_i are the actual and estimated length of the ith leg, respectively. As we know, it is well known the convergence of the Newton–Raphson technique almost entirely depends on the selection of the initial guess and the order of it. We can improve this method by increasing the order of Newton–Raphson. Darvishi and Barati [31] presented a third-order Newton-type method to solve systems of nonlinear equations. In this method, it is not required to calculate second derivatives. Consider the nonlinear equation

$$\mathbf{F}(\mathbf{X}) = \mathbf{0}_{n\times 1} \tag{70}$$

where $\mathbf{F}^{n\times 1}$ is nonlinear function system and $\mathbf{X}$ is a vector of the variables we wish to estimate. They proposed to solve the nonlinear system Eq. (70), the following iteration scheme. Also, they showed that this method has an order of convergence three

$$\mathbf{X}_{m+1} = \mathbf{X}_m - \mathbf{F}'(\mathbf{X}_m)^{-1}\left(\mathbf{F}(\mathbf{X}_m) + \mathbf{F}(\mathbf{X}^*_{m+1})\right) \tag{71}$$

$$\mathbf{X}^*_{m+1} = \mathbf{X}_m - \mathbf{F}'(\mathbf{X}_m)^{-1}\mathbf{F}(\mathbf{X}_m) \tag{72}$$

where $\mathbf{F}'$ is Jacobian matrix and defined by

$$\mathbf{F}'(\mathbf{X}_m) = \frac{\partial \mathbf{F}(\mathbf{X}_m)}{\partial(\mathbf{X}_m)} \tag{73}$$

It should be mentioned that in this study, the stop criteria is $\|\mathbf{X}_{m+1} - \mathbf{X}_m\|_\infty < E_{\max}$. Figure 5 shows the desired trajectory and error between this and modified strategy.

To investigate the performance of the modified method, the trajectory shown in Fig. 5 is used and divided into 201 data points. Table 1 shows the total execution time and the average iteration number for the conventional Newton–Raphson, and our modified method. In this table, for the entire trajectory, the Newton–Raphson is repeated three times using different initial guesses. As can be seen in this table, results of the Newton–Raphson method are significantly dependent on the initial guess. Additionally, using the modified method the total execution time and average iteration number are significantly improved.

In this table, "N" and "t" are the average number of iterations and execution time of the corresponding method, respectively. Next, in another case study, to cover the entire workspace, 201 random data points in the workspace are selected. Figure 6 compares the performance of the modified hybrid method (neural networks and third-order Newton–Raphson), the hybrid method [30] (neural networks and second-order Newton–Raphson) and the Newton–Raphson for four accuracy levels $E_{\max} = 10^{-3}, 10^{-4}, 10^{-5}$ and 10^{-6}. Six random values for the actuator length, q_i^{ac}, resulting in a position and orientation for the MP are selected. This process is repeated 201 times and therefore covers much of the robot workspace. The distributions of the iteration numbers for the mentioned accuracy levels are calculated. A better performance (in terms of execution time) of the employed method results in a distribution closer to the vertical axis. As illustrated for all levels of accuracy, the proposed methodology, modified hybrid method, performs faster compared with the other two aforementioned methods. Therefore, we can claim to have found a near-exact solution to the DKP in a relative small number of iterations. Moreover, Fig. 6 shows that for higher levels of accuracy, the modified hybrid method has better time performance and fewer iterations compared to the two

Table 1 Performance comparison of the modified Hybrid and conventional Newton–Raphson Methods

Precision level	Stop criterion (E_{max})	The modified hybrid method	Conventional Newton–Raphson
1	10^{-12}	Initial guess: automatically calculated by the MLPANN	Initial guess = [0.06, 0.12, 1.12, 0.15, 0.15, 0.11, 0.15] $N = 5.6$ (average of 201 iterations) $t = 0.57$ s (elapsed time for the entire trajectory)
		$N = 3.82$	Initial guess = [0, 0, 1, 0, 0.15, 0] $N = 5.74$ $t = 0.61$ s
		$t = 0.26$ (s)	Initial guess = [0.09, 0.2, 1.2, 0.24, 0.034, 0.24] $N = 871.7$ $t = 32.7$ s

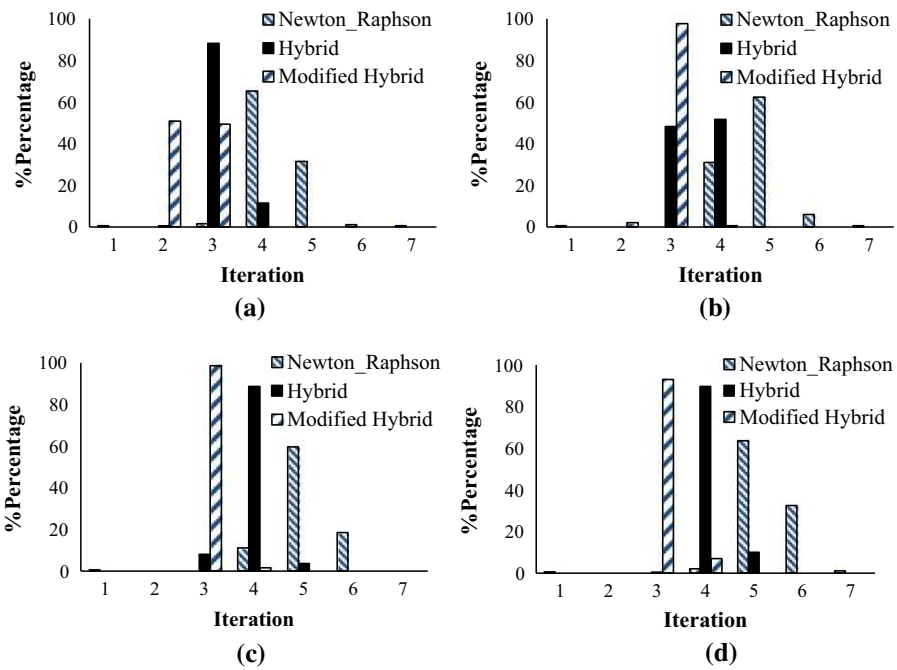

Fig. 6 Distribution of iteration number for four accuracy levels. **a** $E_{max} = 10^{-3}$, **b** $E_{max} = 10^{-4}$, **c** $E_{max} = 10^{-5}$, **d** $E_{max} = 10^{-6}$

others methods. For example, in Fig. 6d, for the modified hybrid method, 93 and 7 % of 201 random points satisfy the fourth accuracy level, $E_{max} = 10^{-6}$, in 3rd and 4th iteration numbers, respectively. However, for the Newton–Raphson method, 66, 30, 3 and 1 % of 201 random points satisfy this criterion in fourth, fifth, sixth and seventh iteration numbers, respectively.

By applying the proposed method, it was demonstrated that replacing the conventional Newton–Raphson algorithm by the third-order counterpart leads to a reduction in the number of iterations required to reach the desired accuracy level and thus a reduction of the DKP analysis time. By reducing the processing time related to solving the DKP, more time can be devoted to

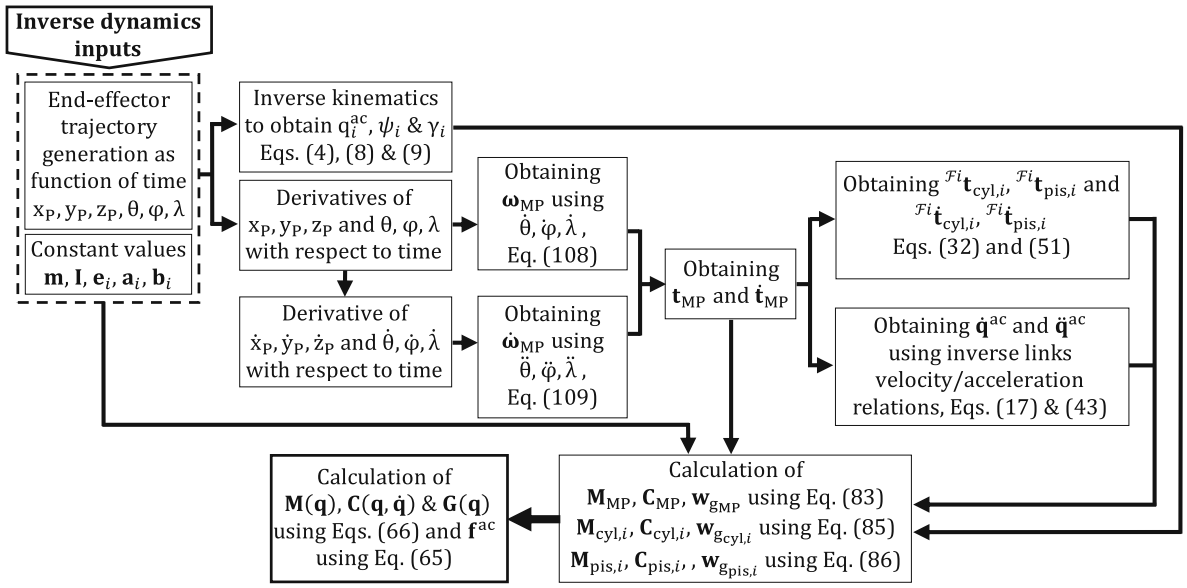

Fig. 7 Computational algorithm for solving the inverse dynamics of the robot

the control calculations. Therefore, more complicated control algorithms with better performances could be implemented. It can be concluded that the proposed method can decrease the iteration number and execution time in comparison with the hybrid method [30] as well as the conventional Newton–Raphson method. Therefore, both goals of finding the nearest exact solution and fast algorithm for the DKP are satisfied.

As stated earlier, the solution outlined in this paper applies to a Gough–Stewart manipulator. Based on the previous sections, a computer program is developed using MATLAB software. Two examples with different initial conditions and applied torques for actuators are simulated and trajectory of this robot is calculated. The results are verified in two ways. First, using inverse dynamics problem, a trajectory for the Gough–Stewart platform is supplied and required motor torques as well as the angular position of actuators as a function of time are calculated. Therefore, the initial conditions of actuator angular positions and velocities can be calculated. If these initial conditions along with torque trajectory, the output of the inverse dynamics problem, are supplied to the direct dynamics problem, then the same trajectory for Gough–Stewart robot must be obtained. Secondly, the results are also verified using a commercial dynamics modeling software. Figures 7 and 8 represent computational algorithm for solving the inverse and direct dynamics of the robot, respectively.

8.1 Specification of the Gough–Stewart platform

The kinematic and dynamic parameters of manipulator are summarized in Table 2.

8.2 Case study 1

In this section, results are verified using a commercial dynamics modeling package. In this simulation, the moving does not rotate, while the center of mass follows a helix curve. Therefore, the trajectory is specified as

$$\theta = \varphi = \lambda = 0 \quad \text{and} \quad \mathbf{p} = \begin{bmatrix} 0.1\cos(\omega t) \\ 1 + 0.01\mathrm{t} \\ 0.1\sin(\omega t) \end{bmatrix}$$

where $\omega = 2.0\,\mathrm{rad/s}$. As shown in Fig. 9, the results of the analytical and commercial software are very close. These results verify the correctness of our mathematical model.

8.3 Case study 2

For the second simulation, the orientation of the MP is rotated about x, while the center of mass moves with a sinusoidal motion. Specifically, the trajectory of the MP is given by

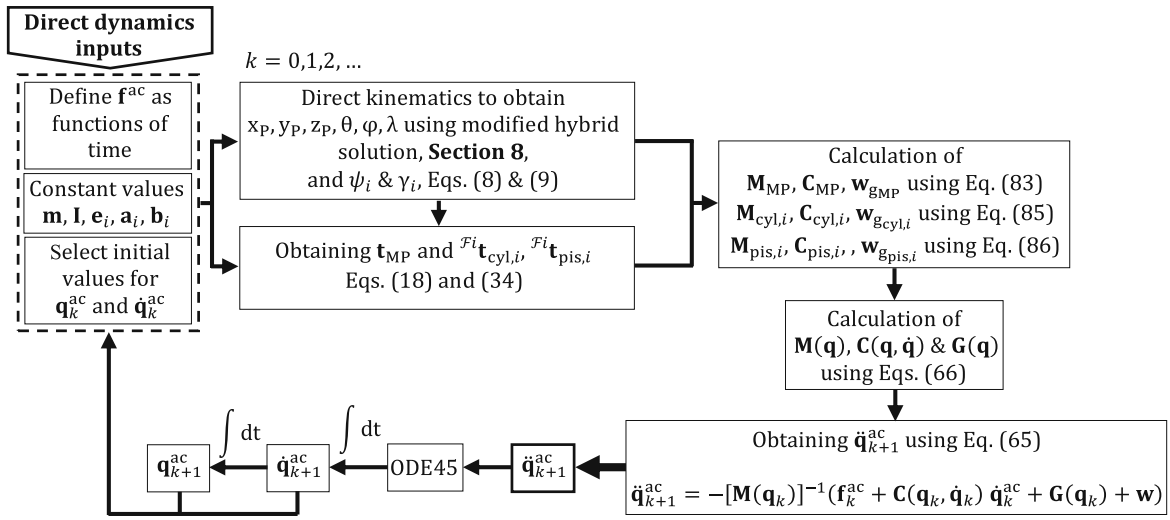

Fig. 8 Computational algorithm for solving the direct dynamics of the robot

Table 2 Physical parameters of the 6-UPS robot

Position vectors of U-joints and S-joints

$a_1 = [0.7071, -7071, 0]^{T_m}$ ${}^{T}b_1 = [0.4830, -0.1294, 0]^{T_m}$

$a_2 = [0.7071, 0.7071, 0]^{T_m}$ ${}^{T}b_2 = [0.4830, 0.1294, 0]^{T_m}$

$a_3 = [0.2588, 0.9659, 0]^{T_m}$ ${}^{T}b_3 = [-0.1294, 0.4830, 0]^{T_m}$

$a_4 = [-0.9659, 0.2588, 0]^{T_m}$ ${}^{T}b_4 = [-0.3536, 0.3536, 0]^{T_m}$

$a_5 = [-0.9659, -0.2588, 0]^{T_m}$ ${}^{T}b_5 = [-0.3536, -0.3536, 0]^{T_m}$

$a_6 = [0.2588, -0.9659, 0]^{T_m}$ ${}^{T}b_6 = [-0.1294, -4830, 0]^{T_m}$

Gravity centers of cylinder and piston for all legs

$e_1 = e_2 = 0.5$ m

Mass of the MP, cylinder and piston of all legs:

$m_{MP} = 1.5\,\text{kg} \quad m_{cyl} = m_{pis} = 0.1\,\text{kg}$

Moments of inertia of cylinder and piston of all legs as well as the MP (in local frames)

$${}^{T}\mathbf{I}_{MP} = \begin{bmatrix} 0.08 & 0 & 0 \\ 0 & 0.08 & 0 \\ 0 & 0 & 0.08 \end{bmatrix} (\text{kg m}^2)$$

$${}^{\mathcal{F}i}\mathbf{I}_{cyl,i} = \begin{bmatrix} 6.25 & 0 & 0 \\ 0 & 6.25 & 0 \\ 0 & 0 & 0 \end{bmatrix} \times 10^{-3}\,(\text{kg m}^2)$$

$${}^{\mathcal{F}i}\mathbf{I}_{pis,i} = \begin{bmatrix} 6.25 & 0 & 0 \\ 0 & 6.25 & 0 \\ 0 & 0 & 0 \end{bmatrix} \times 10^{-3}\,(\text{kg m}^2)$$

$\theta = 0.15 \sin(\omega t)\,, \quad \varphi = \lambda = 0$ and

$$\mathbf{p} = \begin{bmatrix} 0.15 \sin(\omega t) \\ 0.15 \sin(\omega t) \\ 1.0 + 0.15 \sin(\omega t) \end{bmatrix}$$

where $\omega = 0.5$ rad/s. Figure 10 shows the link length in inverse and direct dynamics.

As it is obvious, by reducing execution time related to solving the dynamics equations, more time could be devoted to control calculations. Therefore, more complicated control algorithms with better performances could be implemented [32]. In the Newton–Euler method, all unnecessary constraint forces appear

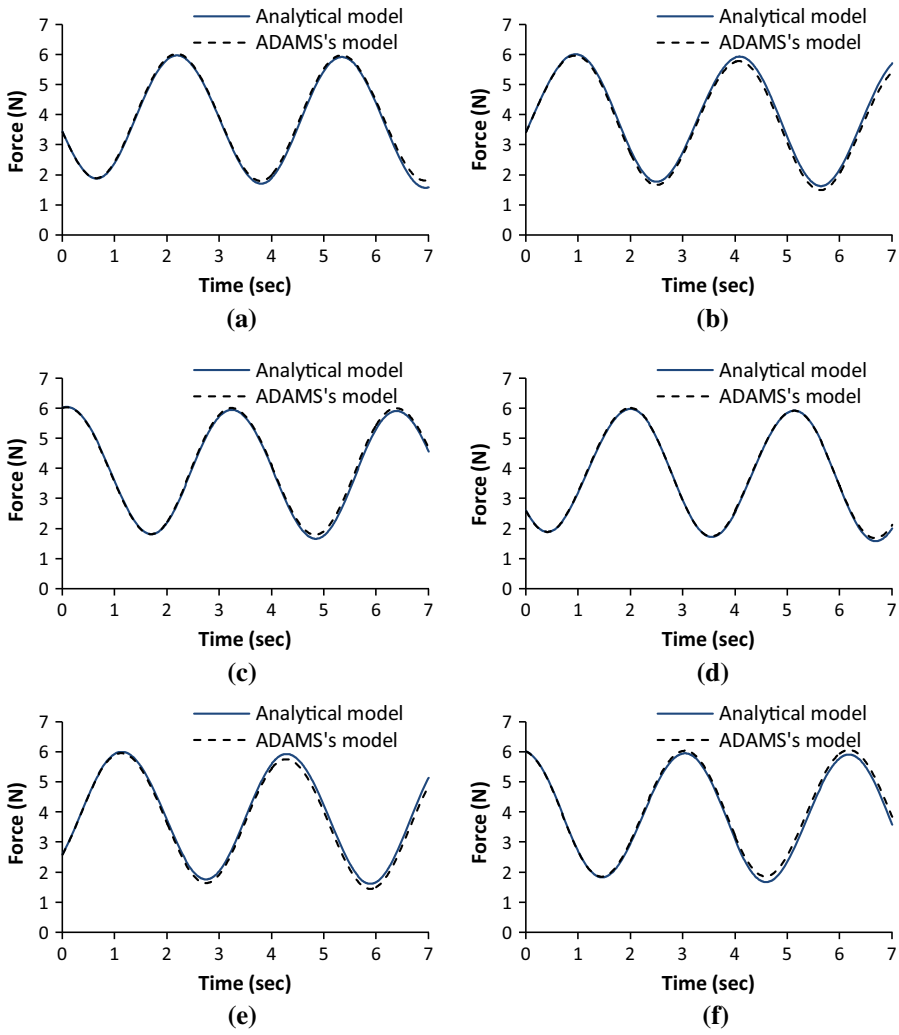

Fig. 9 Input forces at the six prismatic joints in case study 1. **a** Prismatic joint 1, **b** prismatic joint 2, **c** prismatic joint 3, **d** prismatic joint 4, **e** prismatic joint 5, **f** prismatic joint 6

in the robot's dynamic formulations. These unnecessary computations are not essential for control scheme of the robot, and they increase the execution time of the dynamic procedure. Furthermore, the Lagrange method is a strong method and dynamic formulation that is obtained using this method is well structured, but having a large symbolic computation to derive the partial derivatives of the Lagrangian, increases the total execution time of the dynamic procedure [2,17]. Since one of the main goals of the present paper is to reduce execution time, a comparison between execution time for the virtual work and Euler–Lagrange methods is presented.

To have a reasonable comparison, Euler–Lagrange equations are calculated in two cases. The specification of each case is summarized in Table 3. It should be noted that for case 2, calculating partial derivatives of kinetics and potential energy of the robot are very complicated. Therefore, these operations were calculated symbolically. Table 3, compares execution time when a 4-s-long motion trajectory is for the MP as

$$\theta = \lambda = 0.25\sin(2t)\,, \quad \varphi = 0.15\sin(2t) \qquad \text{and}$$

$$\mathbf{p} = \begin{bmatrix} 0.1\sin(2\mathrm{t}) \\ 0.2\sin(2\mathrm{t}) \\ 1.0 + 0.2\sin(2\mathrm{t}) \end{bmatrix} \quad t = 4\,\mathrm{s}$$

As indicated in Table 3, the virtual work method is faster than the Lagrange method. Moreover, Fig. 11 compares the required forces for the six actuators.

In this study, we calculate the dynamic equation of this robot using Euler–Lagrange in two cases to show the better ability of the virtual work method for both

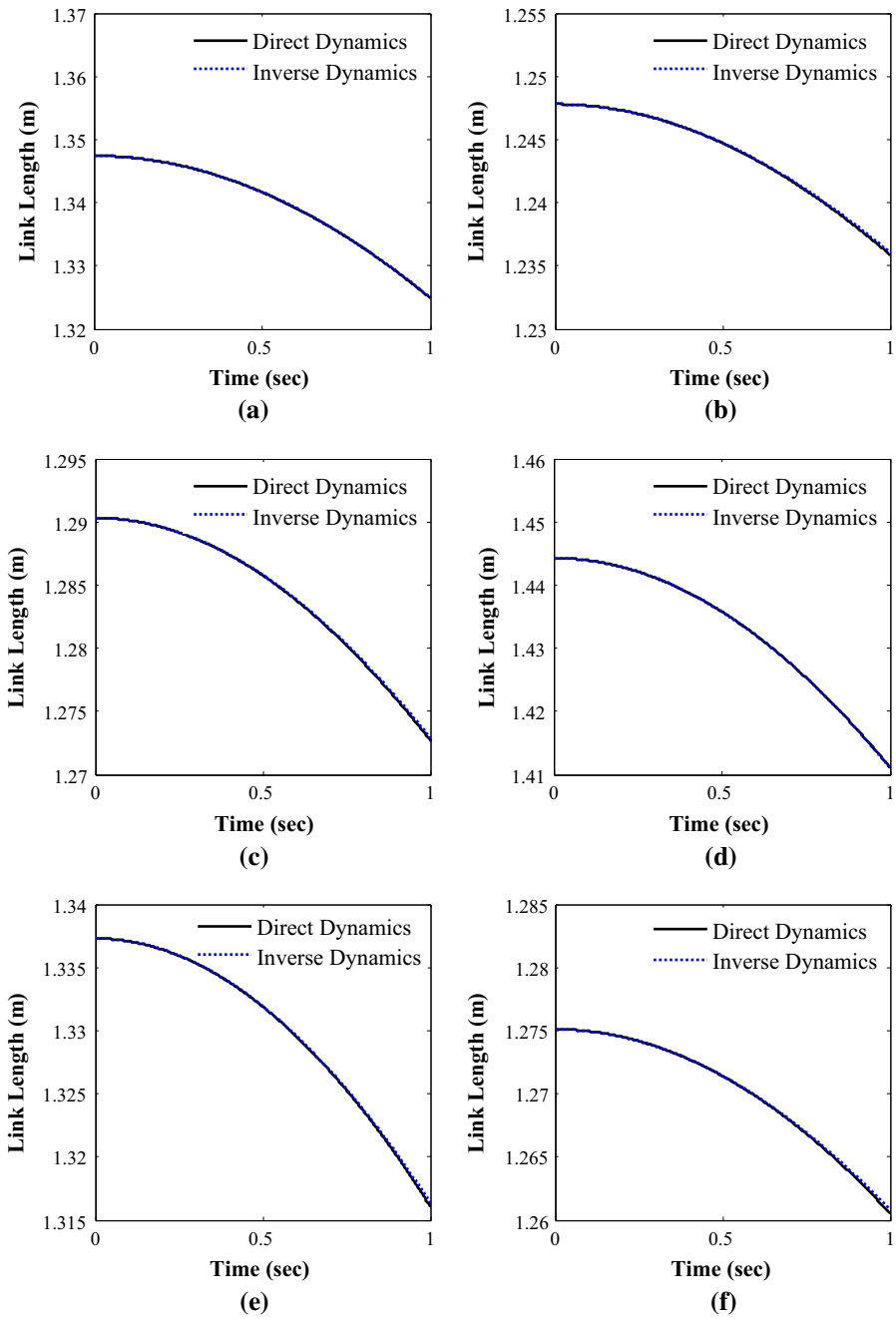

Fig. 10 Input forces at the six prismatic joints in case study 2. **a** Prismatic joint 1, **b** prismatic joint 2, **c** prismatic joint 3, **d** prismatic joint 4, **e** prismatic joint 5, **f** prismatic joint 6

accuracy and execution time (Fig. 11; Table 3). By investigating case 1 and case 2, we can compare the effect of the simplifications on accuracy and execution time. As can be seen, simplification has the direct effect on decreasing the accuracy of the solutions. However, by employing the virtual work methods, without any simplifications, accuracy and execution time are reasonable.

As stated earlier, many methods are employed to obtain the robot's dynamic equations. The complicated partial derivatives, as present in the Lagrange–Euler method, are not utilized in the process of deriv-

Table 3 Performance comparison of Euler–Lagrange and virtual work

Methods	Execution time (s)	Description
Euler–Lagrange		
Case 1	1.15	Distributed mass for MP
		Without considering mass for piston and cylinder of legs
		Obtaining partial derivatives manually
Case 2	14.83	Distributed mass for MP
		Distributed mass for piston and cylinder of each link
		Obtaining partial derivatives symbolically
Virtual work	0.83	Distributed mass for MP
		Distributed mass for piston and cylinder of each link

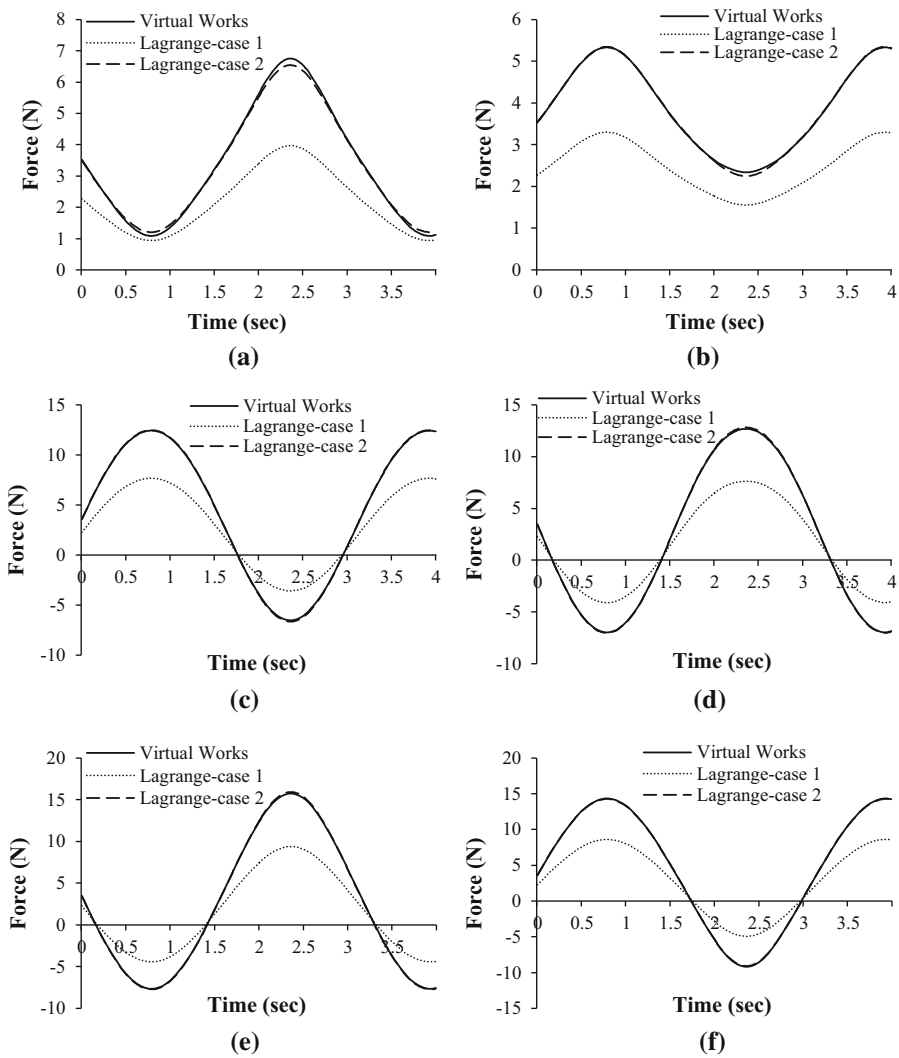

Fig. 11 Required input forces are obtained virtual works and Lagrange methods. **a** Prismatic joint 1, **b** prismatic joint 2, **c** prismatic joint 3, **d** prismatic joint 4, **e** prismatic joint 5, **f** prismatic joint 6

ing the dynamic equations. Additionally, the relatively higher volume of the symbolic computation in the Lagrangian formulation increases the total execution time for the dynamic procedure. Finally, the use of free-body diagrams in Newton–Euler method results in internal moments and forces in the motion equation that are not necessary when simulation and control applications are used [2,3,10,14,17]. More specific differences between the present work and the existing dynamics method are

- To obtain the direct dynamics formulation using the virtual work method requires obtaining the velocity and acceleration transformations between the joint space and Cartesian space. This process is rather complex and not straightforward [17]. However, in the present study, a systematic approach is utilized in obtaining the direct dynamic equations using the virtual work method. To do this, the concept of direct link Jacobian matrices is used to map the twist vector of all rigid bodies to the velocity vector of actuated joints.
- The present approach includes the use of 3×3 transformation matrices rather than the more common 4×4 homogeneous Denavit–Hartenberg transformations as well as the screw theory. This will eliminate the calculation of passive joint velocities and accelerations. Consequently, there is no need to calculate the Jacobian matrices which invert passive joint velocities/accelerations to active joint velocities/accelerations [3,33,34]. Moreover, in the kinematic equations, the passive joints variables are not obtained, and the constraint equations are independent of the passive joints variables. This approach can theoretically lower the execution time of the dynamic solution.
- In some studies, it is assumed that the leg of the 6-UPS robot does not have a spin about its longitudinal axis [13,15,35]. This incorrect assumption results in inaccurate form of the angular velocity/acceleration for the robot's leg. In the present paper, a more precise dynamics formulation is obtained by including the spinning of the legs, consequently the inertia effect, around their axial direction.
- The solution of the direct dynamics requires the solution of the DKP. In the present paper, in an effort to decrease the execution time for analysis of the DKP, a modified hybrid strategy is presented. The new algorithm leads to a reduction in the required iteration numbers to reach the desired accuracy level and subsequently a reduction of the DKP solution time. The reduced time in solving the kinematic equations means more time can be dedicated to more advanced control algorithms. Moreover, this numerical algorithm can be applied to any DKP for serial or parallel robots and obtain the near-exact solutions.
- The aim of this paper is to obtain the motion dynamic equations of the Gough–Stewart robot in a systematic form as well as to offer a workbench on obtaining dynamic of the parallel robots. Although, there exist prior studies on the inverse dynamic solution of Gough–Stewart platform, a few of them have verified dynamic equations using other methods. In the present paper, the dynamic equations are verified by both commercial simulation software and Lagrange method. The other goal of the present study is to reduce execution time in order to implement a model-based controller. To do this, virtual work methodology as well as a modified hybrid strategy is presented. The paper also compares the execution time of the virtual work and well-known Lagrange algorithms.

9 Conclusion

The need to study various control strategies and perform simulation has motivated us to study inverse and direct dynamics problem of the Gough–Stewart parallel robot. A comprehensive model that takes into account all the system parameters such as the MP, cylinder and moving piston of each leg is considered. The methodology involves four basic steps. First, we investigated kinematics solutions. To solve the DKP, an improved hybrid method is used by combining a third-order Newton–Raphson with a Neural Network method. An MLPANN is used to find the initial guess for the Newton–Raphson. The modified hybrid strategy obtains the near-exact solution of the DKP and is computationally efficient. The second step included the calculation of the direct velocity/acceleration analysis using the invariant form for both active and passive joints. We showed that the common assumption of ${}^{\mathcal{F}i}\boldsymbol{\omega}_{\mathrm{Leg},i} \cdot {}^{\mathcal{F}i}\hat{\mathbf{q}}_i^{\mathrm{ac}} = 0$ is not always correct. This assumption does not have a significant effect on the calculated forces by the dynamic solution. Therefore,

it is possible to use this assumption to obtain more simplified equations of motion. In the third step, the concept of direct link Jacobian matrix is utilized to relate the actuator velocities with a related twist of the corresponding leg. In the fourth step, dynamics formulation is presented. The formulation is also implemented in MATLAB software. To demonstrate the methodology, two numerical examples are presented. Results are verified using a commercial dynamics modeling package as well as the Lagrange–Euler method for an inverse dynamics problem. Compared with the traditional Newton–Euler method and the Lagrange formulation, the proposed modeling is more straightforward and systematic resulting in more concise dynamic equations.

Appendix 1

A1.1 Matrices for the moving platform velocity relations

The matrix $\mathbf{J}_{\mathrm{MP}i}$ in Eq. (13) is given below

$$\mathbf{J}_{\mathrm{MP}i} = \left[\mathbf{I}_{3\times3} \; -\mathbf{b}_i \times \mathbf{I}_{3\times3}\right] \quad \text{for} \quad i = 1, \ldots, 6 \tag{74}$$

where

$$\begin{aligned}\mathbf{b}_i \times \mathbf{I}_{3\times3} &= \left[\mathbf{b}_i \times \begin{Bmatrix}1\\0\\0\end{Bmatrix} \; \mathbf{b}_i \times \begin{Bmatrix}0\\1\\0\end{Bmatrix} \; \mathbf{b}_i \times \begin{Bmatrix}0\\0\\1\end{Bmatrix}\right] \\ &= \begin{bmatrix}0 & -b_{iz} & b_{iy}\\ b_{iz} & 0 & -b_{ix}\\ -b_{iy} & b_{ix} & 0\end{bmatrix} \quad \text{for} \quad i = 1, \ldots, 6\end{aligned} \tag{75}$$

and matrix $\mathbf{J}_{\mathrm{MP}}$ in Eq. (17) is given as follows

$$\mathbf{J}_{\mathrm{MP}} = \begin{bmatrix}{}^{\mathcal{F}1}\mathbf{J}_{\mathrm{MP}1(3\times1-6)}\\ \vdots \\ {}^{\mathcal{F}6}\mathbf{J}_{\mathrm{MP}6(3\times1-6)}\end{bmatrix}_{6\times6} \tag{76}$$

A1.2 Matrices for the velocity relations of the robot's legs

The matrix $\mathbf{J}_{\omega i}$ in Eq. (28) is given below

$$\begin{aligned}\mathbf{J}_{\omega i} &= \frac{1}{q_i^{\mathrm{ac}}}\,{}^{\mathcal{F}i}\mathbf{k}_{\mathrm{U}i}\begin{bmatrix}\frac{1}{\cos(\psi_i)}\,{}^{\mathcal{F}i}\mathbf{J}_{\mathrm{MP}i(1\times1-6)}\\ -{}^{\mathcal{F}i}\mathbf{J}_{\mathrm{MP}i(2\times1-6)}\end{bmatrix} \\ &= \frac{1}{q_i^{\mathrm{ac}}}\begin{bmatrix}-{}^{\mathcal{F}i}\mathbf{J}_{\mathrm{MP}i(2\times1-6)}\\ {}^{\mathcal{F}i}\mathbf{J}_{\mathrm{MP}i(1\times1-6)}\\ -\tan(\psi_i)\,{}^{\mathcal{F}i}\mathbf{J}_{\mathrm{MP}i(1\times1-6)}\end{bmatrix}_{3\times6} \\ &\quad \text{for} \quad i = 1, \ldots, 6\end{aligned} \tag{77}$$

and matrices $\mathbf{J}_{v1,i}$ and $\mathbf{J}_{v2,i}$ in Eq. (31) are given below

$$\begin{aligned}\mathbf{J}_{v1,i} &= \frac{\mathrm{e}_1}{\mathrm{q}_i^{\mathrm{ac}}}\begin{bmatrix}{}^{\mathcal{F}i}\mathbf{J}_{\mathrm{MP}i(1-2\times1-6)}\\ \mathbf{0}_{1\times6}\end{bmatrix}_{3\times6}, \\ \mathbf{J}_{v2,i} &= \frac{1}{\mathrm{q}_i^{\mathrm{ac}}}\begin{bmatrix}\left(\mathrm{q}_i^{\mathrm{ac}} - \mathrm{e}_2\right){}^{\mathcal{F}i}\mathbf{J}_{\mathrm{MP}i(1-2\times1-6)}\\ \mathrm{q}_i^{\mathrm{ac}}\,{}^{\mathcal{F}i}\mathbf{J}_{\mathrm{MP}i(3\times1-6)}\end{bmatrix}_{3\times6} \\ &\quad \text{for} \quad i = 1, \ldots, 6\end{aligned} \tag{78}$$

A1.3 Matrices for the moving platform acceleration relations

The matrices in Eqs. (38) and (43) are given as follows

$$\begin{aligned}&\mathbf{N}_i = (\boldsymbol{\omega}_{\mathrm{MP}} \cdot \mathbf{b}_i)\,\mathbf{I}_{3\times3}, \quad \mathbf{m}_i = -(\boldsymbol{\omega}_{\mathrm{MP}} \cdot \boldsymbol{\omega}_{\mathrm{MP}})\,\mathbf{b}_i \\ &\quad \text{for} \quad i = 1, \ldots, 6\end{aligned} \tag{79}$$

and

$$\begin{aligned}\mathbf{N} &= \begin{bmatrix}{}^{\mathcal{F}1}\mathbf{N}_{1(3\times1-3)}\\ \vdots \\ {}^{\mathcal{F}6}\mathbf{N}_{6(3\times1-3)}\end{bmatrix}_{6\times3}, \\ \mathbf{m} &= \begin{Bmatrix}{}^{\mathcal{F}1}m_{1(3)} - q_1^{\mathrm{ac}}\Omega_1\\ \vdots \\ {}^{\mathcal{F}6}m_{6(3)} - q_6^{\mathrm{ac}}\Omega_6\end{Bmatrix}_{6\times1}\end{aligned} \tag{80}$$

where ${}^{\mathcal{F}i}m_{i(k)}$ is the kth element of vector ${}^{\mathcal{F}i}\mathbf{m}_i$ and ${}^{\mathcal{F}i}\mathbf{N}_{i(k\times1-3)}$ is the kth row of ${}^{\mathcal{F}i}\mathbf{N}_i$.

A1.4 Matrices for the acceleration relations of the robot's legs

The matrices in Eqs. (48) and (50) are given as follows

$$\mathbf{\Omega}_{\omega i} = -2\frac{\dot{\mathrm{q}}_i^{\mathrm{ac}}}{q_i^{\mathrm{ac}}}\begin{bmatrix} \mathbf{J}_{\omega i\ (1-2\times 1-6)} \\ -\tan(\psi_i)\,\mathbf{J}_{\omega i\ (2\times 1-6)} \end{bmatrix}_{3\times 6},$$

$$\mathbf{N}_{\omega i} = \frac{1}{\mathrm{q}_i^{\mathrm{ac}}}\begin{bmatrix} -{}^{\mathcal{F}i}\mathbf{N}_{i\ (2\times 1-3)} \\ {}^{\mathcal{F}i}\mathbf{N}_{i\ (1\times 1-3)} \\ -\tan(\psi_i)\,{}^{\mathcal{F}i}\mathbf{N}_{i\ (1\times 1-3)} \end{bmatrix}_{3\times 3}$$

$$\mathbf{m}_{\omega i} = \frac{1}{\mathrm{q}_i^{\mathrm{ac}}}\begin{Bmatrix} -{}^{\mathcal{F}i}m_{i(2)} + \mathrm{q}_i^{\mathrm{ac}}{}^{\mathcal{F}i}\omega_{\mathrm{Leg},iy}\,{}^{\mathcal{F}i}\omega_{\mathrm{Leg},iz} \\ {}^{\mathcal{F}i}m_{i(1)} - \mathrm{q}_i^{\mathrm{ac}}{}^{\mathcal{F}i}\omega_{\mathrm{Leg},ix}\,{}^{\mathcal{F}i}\omega_{\mathrm{Leg},iz} \\ -\tan(\psi_i)\,{}^{\mathcal{F}i}m_{i(1)} - \mathrm{q}_i^{\mathrm{ac}}\left(1+2\tan^2(\psi_i)\right){}^{\mathcal{F}i}\omega_{\mathrm{Leg},ix}\,{}^{\mathcal{F}i}\omega_{\mathrm{Leg},iy} \end{Bmatrix}$$

$$\text{for}\quad i = 1,\ldots,6 \tag{81}$$

and

$$\mathbf{\Omega}_{v1,i} = -2e_1\frac{\dot{q}_i^{\mathrm{ac}}}{q_i^{\mathrm{ac}2}}\begin{bmatrix} {}^{\mathcal{F}i}\mathbf{J}_{\mathrm{MP}i(1-2\times 1-6)} \\ \mathbf{0}_{1\times 6} \end{bmatrix}_{3\times 6},$$

$$\mathbf{\Omega}_{v2,i} = 2e_2\frac{\dot{\mathrm{q}}_i^{\mathrm{ac}}}{q_i^{\mathrm{ac}2}}\begin{bmatrix} {}^{\mathcal{F}i}\mathbf{J}_{\mathrm{MP}i(1-2\times 1-6)} \\ \mathbf{0}_{1\times 6} \end{bmatrix}_{3\times 6}$$

$$\mathbf{N}_{v1,i} = \frac{e_1}{q_i^{\mathrm{ac}}}\begin{bmatrix} {}^{\mathcal{F}i}\mathbf{N}_{i(1-2\times 1-3)} \\ \mathbf{0}_{1\times 3} \end{bmatrix}_{3\times 3},$$

$$\mathbf{N}_{v2,i} = \frac{1}{q_i^{\mathrm{ac}}}\begin{bmatrix} \left(q_i^{\mathrm{ac}} - e_2\right){}^{\mathcal{F}i}\mathbf{N}_{i(1-2\times 1-3)} \\ q_i^{\mathrm{ac}}{}^{\mathcal{F}i}\mathbf{N}_{i(3\times 1-3)} \end{bmatrix}_{3\times 3}$$

$$\mathbf{m}_{v1,i} = \frac{e_1}{q_i^{\mathrm{ac}}}\begin{Bmatrix} {}^{\mathcal{F}i}\mathbf{m}_{i(1-2)} \\ q_i^{\mathrm{ac}}\Omega_i \end{Bmatrix},$$

$$\mathbf{m}_{v2,i} = \frac{1}{q_i^{\mathrm{ac}}}\begin{Bmatrix} \left(q_i^{\mathrm{ac}} - e_2\right){}^{\mathcal{F}i}\mathbf{m}_{i(1-2)} \\ q_i^{\mathrm{ac}}\left({}^{\mathcal{F}i}\mathbf{m}_{i(3)} - e_2\Omega_i\right) \end{Bmatrix}$$

$$\text{for}\quad i = 1,\ldots,6 \tag{82}$$

A1.5 Matrices for equations of motion

The matrices in Eq. (58) are given as follows

$$\mathbf{M}_{\mathrm{MP}} = \begin{bmatrix} -\mathrm{m}_{\mathrm{MP}}\mathbf{J}_{v_{\mathrm{MP}}}^{-1} \\ -{}^{\mathrm{B}}\mathbf{I}_{\mathrm{MP}}\mathbf{J}_{\omega_{\mathrm{MP}}}^{-1} \end{bmatrix}_{6\times 6},$$

$$\mathbf{C}_{\mathrm{MP}} = \begin{bmatrix} -m_{\mathrm{MP}}\mathbf{J}_{v_{\mathrm{Cor,MP}}} \\ -{}^{\mathrm{B}}\mathbf{I}_{\mathrm{MP}}\mathbf{J}_{\omega_{\mathrm{Cor,MP}}} - (\boldsymbol{\omega}_{\mathrm{MP}}\times\mathbf{I}_{3\times 3})\,{}^{\mathrm{B}}\mathbf{I}_{\mathrm{MP}}\mathbf{J}_{\omega_{\mathrm{MP}}}^{-1} \end{bmatrix}_{6\times 6}$$

$$\mathbf{w}_{g_{\mathrm{MP}}} = \begin{Bmatrix} m_{\mathrm{MP}}\mathbf{g} \\ \mathbf{0}_{3\times 1} \end{Bmatrix},\quad \mathbf{w}_{\mathrm{ext}} = \begin{Bmatrix} \mathbf{f}_{\mathrm{ext}} \\ \mathbf{n}_{\mathrm{ext}} \end{Bmatrix} \tag{83}$$

where

$$\mathbf{J}_{v_{\mathrm{MP}}}^{-1} = \mathbf{J}_{\mathrm{MP}(1-3)\times(1-6)}^{-1},\quad \mathbf{J}_{\omega_{\mathrm{MP}}}^{-1} = \mathbf{J}_{\mathrm{MP}(4-6)\times(1-6)}^{-1}$$

$$\mathbf{J}_{v_{\mathrm{Cor,MP}}} = \mathbf{J}_{\mathrm{Cor,MP}(1-3)\times(1-6)},$$
$$\mathbf{J}_{\omega_{\mathrm{Cor,MP}}} = \mathbf{J}_{\mathrm{Cor,MP}(4-6)\times(1-6)} \tag{84}$$

and matrices in Eq. (61) are given as follows

$$\mathbf{M}_{\mathrm{cyl},i} = \begin{bmatrix} -\mathrm{m}_{\mathrm{cyl},i}\mathbf{J}_{v1,i}\mathbf{J}_{\mathrm{MP}}^{-1} \\ -{}^{\mathcal{F}i}\mathbf{I}_{\mathrm{cyl},i}\mathbf{J}_{\omega i}\mathbf{J}_{\mathrm{MP}}^{-1} \end{bmatrix}_{6\times 6},$$

$$\mathbf{w}_{g_{\mathrm{cyl},i}} = \begin{Bmatrix} \mathrm{m}_{\mathrm{cyl},i}\,{}^{\mathcal{F}i}_{\mathrm{B}}\mathbf{R}\,\mathbf{g} \\ \mathbf{0}_{3\times 1} \end{Bmatrix}$$

$$\mathbf{C}_{\mathrm{cyl},i} = \begin{bmatrix} -\mathrm{m}_{\mathrm{cyl},i}\mathbf{J}_{v_{\mathrm{Cor,cyl},i}} \\ -{}^{\mathcal{F}i}\mathbf{I}_{\mathrm{cyl},i}\mathbf{J}_{\omega_{\mathrm{Cor,cyl},i}} - \left({}^{\mathcal{F}i}\boldsymbol{\omega}_{\mathrm{Leg},i}\times\mathbf{I}_{3\times 3}\right){}^{\mathcal{F}i}\mathbf{I}_{\mathrm{cyl},i}\mathbf{J}_{\omega i}\mathbf{J}_{\mathrm{MP}}^{-1} \end{bmatrix}_{6\times 6}$$

$$\text{for}\quad i = 1,\ldots,6 \tag{85}$$

and

$$\mathbf{M}_{\mathrm{pis},i} = \begin{bmatrix} -\mathrm{m}_{\mathrm{pis},i}\mathbf{J}_{v2,i}\mathbf{J}_{\mathrm{MP}}^{-1} \\ -{}^{\mathcal{F}i}\mathbf{I}_{\mathrm{pis},i}\mathbf{J}_{\omega i}\mathbf{J}_{\mathrm{MP}}^{-1} \end{bmatrix}_{6\times 6},$$

$$\mathbf{w}_{g_{\mathrm{pis},i}} = \begin{Bmatrix} \mathrm{m}_{\mathrm{pis},i}\,{}^{\mathcal{F}i}_{\mathrm{B}}\mathbf{R}\,\mathbf{g} \\ \mathbf{0}_{3\times 1} \end{Bmatrix}$$

$$\mathbf{C}_{\mathrm{pis},i} = \begin{bmatrix} -\mathrm{m}_{\mathrm{pis},i}\mathbf{J}_{v_{\mathrm{Cor,pis},i}} \\ -{}^{\mathcal{F}i}\mathbf{I}_{\mathrm{pis},i}\mathbf{J}_{\omega_{\mathrm{Cor,pis},i}} - \left({}^{\mathcal{F}i}\boldsymbol{\omega}_{\mathrm{Leg},i}\times\mathbf{I}_{3\times 3}\right){}^{\mathcal{F}i}\mathbf{I}_{\mathrm{pis},i}\mathbf{J}_{\omega i}\mathbf{J}_{\mathrm{MP}}^{-1} \end{bmatrix}_{6\times 6}$$

$$\text{for}\quad i = 1,\ldots,6 \tag{86}$$

where

$$\mathbf{J}_{v_{\mathrm{Cor,cyl},i}} = \mathbf{J}_{\mathrm{Cor,cyl},i(1-3)\times(1-6)},$$
$$\mathbf{J}_{\omega_{\mathrm{Cor,cyl},i}} = \mathbf{J}_{\mathrm{Cor,cyl},i(4-6)\times(1-6)}$$
$$\mathbf{J}_{v_{\mathrm{Cor,pis},i}} = \mathbf{J}_{\mathrm{Cor,pis},i(1-3)\times(1-6)},$$
$$\mathbf{J}_{\omega_{\mathrm{Cor,pis},i}} = \mathbf{J}_{\mathrm{Cor,pis},i(4-6)\times(1-6)}$$
$$\text{for}\quad i = 1,\ldots,6 \tag{87}$$

Appendix 2

To obtain the overall direct acceleration relation, Eq. (44), as a function of $\ddot{\mathbf{q}}^{\mathrm{ac}}$ and $\dot{\mathbf{q}}^{\mathrm{ac}}$, vectors $\boldsymbol{\omega}_{\mathrm{MP}}$

and $\mathbf{m}$ must be obtained as functions of $\dot{\mathbf{q}}^{\mathrm{ac}}$. Using Eq. (18), $\boldsymbol{\omega}_{\mathrm{MP}}$ can be obtained as function of $\ddot{\mathbf{q}}^{\mathrm{ac}}$ as below

$$\boldsymbol{\omega}_{\mathrm{MP}} = \mathbf{J}^{-1}_{\mathrm{MP}_{(4-6)\times 6}} \dot{\mathbf{q}}^{\mathrm{ac}} \tag{88}$$

Therefore, using Eq. (88), we can write

$$\boldsymbol{\omega}_{\mathrm{MP}} \cdot \boldsymbol{\omega}_{\mathrm{MP}} = \|\boldsymbol{\omega}_{\mathrm{MP}}\|^2 = \boldsymbol{\xi}_{1\times 6} \dot{\mathbf{q}}^{\mathrm{ac}} \tag{89}$$

where

$$\boldsymbol{\xi}_{1\times 6} = \sum_{j=1}^{3} \mathbf{J}^{-1}_{\mathrm{MP}(4-6)\times 6\ (\mathrm{row}\ j)} \left(\dot{\mathbf{q}}^{\mathrm{ac}^{\mathrm{T}}} \mathbf{J}^{-\mathrm{T}}_{\mathrm{MP}(4-6)\times 6\ (\mathrm{row}\ j)} \right) \tag{90}$$

By substituting Eqs. (89) into (79), vectors $\mathbf{m}_i$ and ${}^{\mathcal{F}i}\mathbf{m}_i$ can be rewritten in terms of $\dot{\mathbf{q}}^{\mathrm{ac}}$ as follows

$$\begin{aligned} \mathbf{m}_i &= -\left(\boldsymbol{\omega}_{\mathrm{MP}} \cdot \boldsymbol{\omega}_{\mathrm{MP}}\right) \mathbf{b}_i = \boldsymbol{\eta}_{i_{3\times 6}} \dot{\mathbf{q}}^{\mathrm{ac}} \\ {}^{\mathcal{F}i}\mathbf{m}_i &= {}^{\mathcal{F}i}\boldsymbol{\eta}_{i_{3\times 6}} \dot{\mathbf{q}}^{\mathrm{ac}} \qquad \text{for} \quad i = 1, \ldots, 6 \end{aligned} \tag{91}$$

where $\boldsymbol{\eta}_{i_{3\times 6}} = -\mathbf{b}_{i_{3\times 1}} \boldsymbol{\xi}_{1\times 6}$ and ${}^{\mathcal{F}i}\boldsymbol{\eta}_{i_{3\times 6}} = {}^{\mathcal{F}i}_{\mathrm{B}}\mathbf{R}\boldsymbol{\eta}_{i_{3\times 6}}$. Also, value of Ω_i, Eq. (41), can be derived as a function of $\dot{\mathbf{q}}^{\mathrm{ac}}$ using Eq. (33) as

$$\Omega_i = -\left({}^{\mathcal{F}i}\omega^2_{\mathrm{Leg},ix} + {}^{\mathcal{F}i}\omega^2_{\mathrm{Leg},iy} \right) = \boldsymbol{\zeta}_{i1\times 6} \dot{\mathbf{q}}^{\mathrm{ac}} \qquad \text{for} \quad i = 1, \ldots, 6 \tag{92}$$

where

$$\boldsymbol{\zeta}_{i_{1\times 6}} = -\sum_{j=1}^{2} \left[\mathbf{J}_{\omega i}\ \mathbf{J}^{-1}_{\mathrm{MP}} \right]_{(\mathrm{row}\ j)} \left(\dot{\mathbf{q}}^{\mathrm{ac}^{\mathrm{T}}} \left[\mathbf{J}_{\omega i}\ \mathbf{J}^{-1}_{\mathrm{MP}} \right]^{\mathrm{T}}_{(\mathrm{row}\ j)} \right) \qquad \text{for} \quad i = 1, \ldots, 6 \tag{93}$$

Consequently, substituting Eqs. (91) and (92) into Eq. (80), vector $\mathbf{m}$ is rewritten as a function of $\dot{\mathbf{q}}^{\mathrm{ac}}$ as follows

$$\mathbf{m} = \boldsymbol{\Lambda}_{6\times 6} \dot{\mathbf{q}}^{\mathrm{ac}} \tag{94}$$

where vector $\mathbf{m}$ is shown in "Appendix 1" and matrix $\boldsymbol{\Lambda}_{6\times 6}$ is obtained as below

$$\boldsymbol{\Lambda}_{6\times 6} = \begin{bmatrix} {}^{\mathcal{F}1}\boldsymbol{\eta}_{1\ 3\times(1-6)} - \mathrm{q}^{\mathrm{ac}}_1 \boldsymbol{\zeta}_1 \\ \vdots \\ {}^{\mathcal{F}6}\boldsymbol{\eta}_{6\ 3\times(1-6)} - \mathrm{q}^{\mathrm{ac}}_6 \boldsymbol{\zeta}_6 \end{bmatrix}_{6\times 6} \tag{95}$$

Therefore, using Eq. (44), we can write

$$\begin{aligned} &\mathbf{J}_{\mathrm{Cor,\ MP}}\left(\mathbf{q}^{\mathrm{ac}}, \dot{\mathbf{q}}^{\mathrm{ac}}\right) \\ &\quad = -\mathbf{J}^{-1}_{\mathrm{MP}} \left(\mathbf{N}\, \mathbf{J}^{-1}_{\mathrm{MP}(4-6)\times 6} + \boldsymbol{\Lambda}_{6\times 6} \right) \end{aligned} \tag{96}$$

where matrix $\mathbf{N}$ is shown in "Appendix 1."

Appendix 3

A3.1 Obtaining the values of $\ddot{\gamma}_i$ and $\ddot{\psi}_i$

As stated earlier, the cross product of both sides of Eq. (39) with unit vector ${}^{\mathcal{F}i}\hat{\mathbf{q}}^{\mathrm{ac}}_i$ leads to obtain values of $\ddot{\gamma}_i$ and $\ddot{\psi}_i$. This yields

$$\begin{aligned} &{}^{\mathcal{F}i}\hat{\mathbf{q}}^{\mathrm{ac}}_i \times \left({}^{\mathcal{F}i}\dot{\boldsymbol{\omega}}_{\mathrm{Leg},i} \times^{\mathcal{F}i} \hat{\mathbf{q}}^{\mathrm{ac}}_i \right) = \frac{1}{\mathrm{q}^{\mathrm{ac}}_i} \left({}^{\mathcal{F}i}\hat{\mathbf{q}}^{\mathrm{ac}}_i \times^{\mathcal{F}i} \dot{\boldsymbol{v}}_{\mathrm{S}i} \right) \\ &\quad - 2\frac{\dot{\mathrm{q}}^{\mathrm{ac}}_i}{\mathrm{q}^{\mathrm{ac}}_i} \left({}^{\mathcal{F}i}\hat{\mathbf{q}}^{\mathrm{ac}}_i \times \left({}^{\mathcal{F}i}\boldsymbol{\omega}_{\mathrm{Leg},i} \times^{\mathcal{F}i} \hat{\mathbf{q}}^{\mathrm{ac}}_i \right) \right) \\ &\quad - {}^{\mathcal{F}i}\hat{\mathbf{q}}^{\mathrm{ac}}_i \times \left({}^{\mathcal{F}i}\boldsymbol{\omega}_{\mathrm{Leg},i} \times \left({}^{\mathcal{F}i}\boldsymbol{\omega}_{\mathrm{Leg},i} \times^{\mathcal{F}i} \hat{\mathbf{q}}^{\mathrm{ac}}_i \right) \right) \\ &\quad \text{for} \quad i = 1, \ldots, 6 \end{aligned} \tag{97}$$

where ${}^{\mathcal{F}i}\hat{\mathbf{q}}^{\mathrm{ac}}_i \times \left({}^{\mathcal{F}i}\dot{\boldsymbol{\omega}}_{\mathrm{Leg},i} \times^{\mathcal{F}i} \hat{\mathbf{q}}^{\mathrm{ac}}_i \right) = \left\{ {}^{\mathcal{F}i}\dot{\omega}_{\mathrm{Leg},ix}\ {}^{\mathcal{F}i}\dot{\omega}_{\mathrm{Leg},iy}\ 0 \right\}^{\mathrm{T}}$. Using Eq. (28) yield

$$\begin{aligned} &{}^{\mathcal{F}i}\hat{\mathbf{q}}^{\mathrm{ac}}_i \times \left({}^{\mathcal{F}i}\boldsymbol{\omega}_{\mathrm{Leg},i} \times^{\mathcal{F}i} \hat{\mathbf{q}}^{\mathrm{ac}}_i \right) \\ &\quad = \begin{bmatrix} \mathbf{J}_{\omega i\ (1-2\ \times\ 1-6)} \\ \mathbf{0}_{1\times 6} \end{bmatrix}_{3\times 6} \mathbf{t}_{\mathrm{MP}} \qquad \text{for } i = 1, \ldots, 6 \end{aligned} \tag{98}$$

where $\mathbf{J}_{\omega i(m-n\times 1-6)}$ is a matrix composed of mth to nth rows of matrix $\mathbf{J}_{\omega i}$ and

$$\begin{aligned} &{}^{\mathcal{F}i}\hat{\mathbf{q}}^{\mathrm{ac}}_i \times \left({}^{\mathcal{F}i}\boldsymbol{\omega}_{\mathrm{Leg},i} \times \left({}^{\mathcal{F}i}\boldsymbol{\omega}_{\mathrm{Leg},i} \times^{\mathcal{F}i} \hat{\mathbf{q}}^{\mathrm{ac}}_i \right) \right) \\ &\quad = \begin{Bmatrix} -{}^{\mathcal{F}i}\omega_{\mathrm{Leg},iy}\ {}^{\mathcal{F}i}\omega_{\mathrm{Leg},iz} \\ {}^{\mathcal{F}i}\omega_{\mathrm{Leg},ix}\ {}^{\mathcal{F}i}\omega_{\mathrm{Leg},iz} \\ 0 \end{Bmatrix} \qquad \text{for } i = 1, \ldots, 6 \end{aligned} \tag{99}$$

Also, using Eq. (42) yield

$$\begin{aligned} {}^{\mathcal{F}i}\hat{\mathbf{q}}^{\mathrm{ac}}_i \times^{\mathcal{F}i} \dot{\boldsymbol{v}}_{\mathrm{S}i} &= \begin{bmatrix} -{}^{\mathcal{F}i}\mathbf{J}_{\mathrm{MP}i\ (2\ \times\ 1-6)} \\ {}^{\mathcal{F}i}\mathbf{J}_{\mathrm{MP}i\ (1\ \times\ 1-6)} \\ \mathbf{0}_{1\times 6} \end{bmatrix} \dot{\mathbf{t}}_{\mathrm{MP}} \\ &\quad + \begin{bmatrix} -{}^{\mathcal{F}i}\mathbf{N}_{i\ (2\ \times\ 1-3)} \\ {}^{\mathcal{F}i}\mathbf{N}_{i\ (1\ \times\ 1-3)} \\ \mathbf{0}_{1\times 3} \end{bmatrix} \boldsymbol{\omega}_{\mathrm{MP}} \\ &\quad + \begin{Bmatrix} -{}^{\mathcal{F}i}\mathrm{m}_{i\ (2)} \\ {}^{\mathcal{F}i}\mathrm{m}_{i\ (1)} \\ 0 \end{Bmatrix} \qquad \text{for } i = 1, \ldots, 6 \end{aligned} \tag{100}$$

Substituting Eqs. (47) and (98)–(100) into (97), as well as substituting values of $\dot{\psi}_i$ and $\dot{\gamma}_i$ as functions of components of vector ${}^{\mathcal{F}i}\boldsymbol{\omega}_{\mathrm{Leg},i}$ as shown in Eq. (22), yield

$$\begin{Bmatrix} \ddot{\psi}_i \\ \ddot{\gamma}_i \end{Bmatrix} = \frac{1}{\mathrm{q}^{\mathrm{ac}}_i} \left(\begin{bmatrix} -{}^{\mathcal{F}i}\mathbf{J}_{\mathrm{MP}i\ (2\ \times\ 1-6)} \\ \frac{1}{\cos(\psi_i)}\, {}^{\mathcal{F}i}\mathbf{J}_{\mathrm{MP}i\ (1\ \times\ 1-6)} \end{bmatrix} \dot{\mathbf{t}}_{\mathrm{MP}} \right.$$

$$+\left[\begin{array}{c} -{}^{\mathcal{F}i}\mathbf{N}_{i\ (2\times 1-3)} \\ \frac{1}{\cos(\psi_i)}\,{}^{\mathcal{F}i}\mathbf{N}_{i\ (1\times 1-3)} \end{array}\right]\boldsymbol{\omega}_{\mathrm{MP}}+\left\{\begin{array}{c} -{}^{\mathcal{F}i}\mathrm{m}_{i\ (2)} \\ \frac{1}{\cos(\psi_i)}\,{}^{\mathcal{F}i}\mathrm{m}_{i\ (1)} \end{array}\right\}\Bigg)$$
$$-2\frac{\dot{\mathrm{q}}_i^{\mathrm{ac}}}{\mathrm{q}_i^{\mathrm{ac}}}\left[\begin{array}{c} \mathbf{J}_{\omega i\ (1\times 1-6)} \\ \frac{1}{\cos(\psi_i)}\mathbf{J}_{\omega i\ (2\times 1-6)} \end{array}\right]_{3\times 6}\mathbf{t}_{\mathrm{MP}}$$
$$-\left\{\begin{array}{cc} -{}^{\mathcal{F}i}\omega_{\mathrm{Leg},iy} & {}^{\mathcal{F}i}\omega_{\mathrm{Leg},iz} \\ \frac{2}{\cos(\psi_i)}\,{}^{\mathcal{F}i}\omega_{\mathrm{Leg},ix} & {}^{\mathcal{F}i}\omega_{\mathrm{Leg},iz} \end{array}\right\}\quad \text{for } i=1,\ \ldots,\ 6 \tag{101}$$

Therefore, by substituting Eqs. (101) into (47), vector ${}^{\mathcal{F}i}\dot{\boldsymbol{\omega}}_{\mathrm{Leg},i}$, will be rewritten in terms of the end-effector acceleration and velocity vectors in compact form as shown in Eq. (48).

A3.2 Obtaining the matrices $J_{Cor,cyl,i}$ and $J_{Cor,pis,i}$

To derive the overall acceleration vectors of each leg in terms of $\ddot{\mathbf{q}}^{\mathrm{ac}}$ and $\dot{\mathbf{q}}^{\mathrm{ac}}$, the vectors of $\mathbf{m}_{\omega i}$, $\mathbf{m}_{v1,i}$ and $\mathbf{m}_{v2,i}$ should be obtained as function of $\dot{\mathbf{q}}^{\mathrm{ac}}$. Similar to Eq. (92), we can write

$${}^{\mathcal{F}i}\omega_{\mathrm{Leg},i\ m}\ {}^{\mathcal{F}i}\omega_{\mathrm{Leg},i\ n}=\boldsymbol{\zeta}_i^{mn}{}_{1\times 6}\,\dot{\mathbf{q}}^{\mathrm{ac}}\quad \text{for}\quad i=1,\ \ldots,\ 6 \tag{102}$$

where

$$\boldsymbol{\zeta}_i^{mn}=\left[\mathbf{J}_{\omega i}\ \mathbf{J}_{\mathrm{MP}}^{-1}\right]_{(\mathrm{row}\ m)}\left(\dot{\mathbf{q}}^{\mathrm{ac}^{\mathrm{T}}}\left[\mathbf{J}_{\omega i}\ \mathbf{J}_{\mathrm{MP}}^{-1}\right]_{(\mathrm{row}\ n)}^{\mathrm{T}}\right)\ \text{for}\ i=1,\ \ldots,\ 6 \tag{103}$$

By utilizing Eqs. (91), (92) and (102), the vectors $\mathbf{m}_{\omega i}$, $\mathbf{m}_{v1,i}$ and $\mathbf{m}_{v2,i}$ from Eqs. (81) and (82) can be obtained as functions of $\dot{\mathbf{q}}^{\mathrm{ac}}$ as follows

$$\mathbf{m}_{\omega i}=\boldsymbol{\Lambda}_{\omega i}\dot{\mathbf{q}}^{\mathrm{ac}},\ \mathbf{m}_{v1,i}=\boldsymbol{\Lambda}_{v1,i}\dot{\mathbf{q}}^{\mathrm{ac}},$$
$$\mathbf{m}_{v2,\ i}=\boldsymbol{\Lambda}_{v2,i}\dot{\mathbf{q}}^{\mathrm{ac}}\quad \text{for}\quad i=1,\ldots,6 \tag{104}$$

where

$$\boldsymbol{\Lambda}_{\omega i}=\frac{1}{\mathrm{q}_i^{\mathrm{ac}}}\left[\begin{array}{c} -{}^{\mathcal{F}i}\boldsymbol{\eta}_{i_{2\times(1-6)}}+q_i^{\mathrm{ac}}\boldsymbol{\zeta}_i^{yz}{}_{1\times 6} \\ {}^{\mathcal{F}i}\boldsymbol{\eta}_{i\ 1\times(1-6)}-\mathrm{q}_i^{\mathrm{ac}}\ \boldsymbol{\zeta}_i^{xz}{}_{1\times 6} \\ -\tan(\psi_i)\,{}^{\mathcal{F}i}\ \boldsymbol{\eta}_{i\ 1\times(1-6)}-q_i^{\mathrm{ac}}\left(1+2\tan^2(\psi_i)\right)\boldsymbol{\zeta}_i^{xy}{}_{1\times 6} \end{array}\right]_{3\times 6}$$
$$\boldsymbol{\Lambda}_{v1,i}=\frac{\mathrm{e}_1}{\mathrm{q}_i^{\mathrm{ac}}}\left[\begin{array}{c} {}^{\mathcal{F}i}\boldsymbol{\eta}_{i\ (1-2\ \times\ 1-6)} \\ \mathrm{q}_i^{\mathrm{ac}}\ \boldsymbol{\zeta}_{i_{1\times 6}} \end{array}\right]_{3\times 6},$$
$$\boldsymbol{\Lambda}_{v2,i}=\frac{1}{\mathrm{q}_i^{\mathrm{ac}}}\left[\begin{array}{c} \left(\mathrm{q}_i^{\mathrm{ac}}-\mathrm{e}_2\right){}^{\mathcal{F}i}\ \boldsymbol{\eta}_{i\ (1-2\ \times\ 1-6)} \\ \mathrm{q}_i^{\mathrm{ac}}\left({}^{\mathcal{F}i}\boldsymbol{\eta}_{i\ (3\times 1-6)}-\mathrm{e}_2\boldsymbol{\zeta}_{i_{1\times 6}}\right) \end{array}\right]_{3\times 6}$$
$$\text{for}\quad i=1,\ldots,6 \tag{105}$$

Therefore, the overall direct link acceleration relations can be derived in terms of $\ddot{\mathbf{q}}^{\mathrm{ac}}$ and $\dot{\mathbf{q}}^{\mathrm{ac}}$ as shown Eq. (53) by substituting vectors $\boldsymbol{\omega}_{\mathrm{MP}}$ and $\mathbf{t}_{\mathrm{MP}}$ from Eq. (18) and vector $\dot{\mathbf{t}}_{\mathrm{MP}}$ from Eq. (45) as well as vectors $\mathbf{m}_{\omega i}$, $\mathbf{m}_{v1,i}$ and $\mathbf{m}_{v2,i}$ from Eq. (104) into Eqs. (48) and (50). Consequently, matrices $\mathbf{J}_{\mathrm{Cor,cyl,i}}$ and $\mathbf{J}_{\mathrm{Cor,pis,i}}$ can be obtained as follows

$$\mathbf{J}_{\mathrm{Cor,cyl},i}=\left[\begin{array}{c} \mathbf{J}_{v1,i}\mathbf{J}_{\mathrm{Cor,MP}}+\boldsymbol{\Omega}_{v1,i}\mathbf{J}_{\mathrm{MP}}^{-1}+\mathbf{N}_{v1,i}\mathbf{J}_{\mathrm{MP}(4-6)\times 6}^{-1}+\boldsymbol{\Lambda}_{v1,i} \\ \mathbf{J}_{\omega i}\mathbf{J}_{\mathrm{Cor,MP}}+\boldsymbol{\Omega}_{\omega i}\mathbf{J}_{\mathrm{MP}}^{-1}+\mathbf{N}_{\omega i}\mathbf{J}_{\mathrm{MP}(4-6)\times 6}^{-1}+\boldsymbol{\Lambda}_{\omega i} \end{array}\right]$$
$$\mathbf{J}_{\mathrm{Cor,pis},i}=\left[\begin{array}{c} \mathbf{J}_{v2,i}\mathbf{J}_{\mathrm{Cor,MP}}+\boldsymbol{\Omega}_{v2,i}\mathbf{J}_{\mathrm{MP}}^{-1}+\mathbf{N}_{v2,i}\mathbf{J}_{\mathrm{MP}(4-6)\times 6}^{-1}+\boldsymbol{\Lambda}_{v2,i} \\ \mathbf{J}_{\omega i}\mathbf{J}_{\mathrm{Cor,MP}}+\boldsymbol{\Omega}_{\omega i}\mathbf{J}_{\mathrm{MP}}^{-1}+\mathbf{N}_{\omega i}\mathbf{J}_{\mathrm{MP}(4-6)\times 6}^{-1}+\boldsymbol{\Lambda}_{\omega i} \end{array}\right]$$
$$\text{for}\ \ i=1,\ldots,6 \tag{106}$$

Appendix 4

The angular velocity of the MP can be derived as function of three angular velocities contain derivatives of three Euler angles θ, φ and λ, as follows

$$\boldsymbol{\omega}_{\mathrm{MP}}=\dot{\theta}\hat{\mathbf{i}}+\dot{\varphi}\hat{\mathbf{j}}'+\dot{\lambda}\hat{\mathbf{k}}''$$
$$=\dot{\theta}\hat{\mathbf{i}}+\dot{\varphi}\mathbf{R}\,(\mathrm{x},\theta)\,\hat{\mathbf{j}}+\dot{\lambda}\mathbf{R}\,(\mathrm{x},\theta)\,\mathbf{R}\,(\mathrm{y},\varphi)\,\hat{\mathbf{k}} \tag{107}$$

where $\hat{\mathbf{i}}$, $\hat{\mathbf{j}}$ and $\hat{\mathbf{k}}$ are unit vectors along x-, y- and z-axes of the fixed coordinate frame {B} as well as $\dot{\theta}$, $\dot{\varphi}$ and $\dot{\lambda}$ are the angular velocities about x-, y'- and z''-axes, respectively. Also, $\hat{\mathbf{j}}'$ and $\hat{\mathbf{k}}''$ are the unit vectors along rotated y'- and z''-axes, respectively (for more details see Fig. 12).

Therefore, Eqs. (107), (97) can be rewritten as matrix form as follows

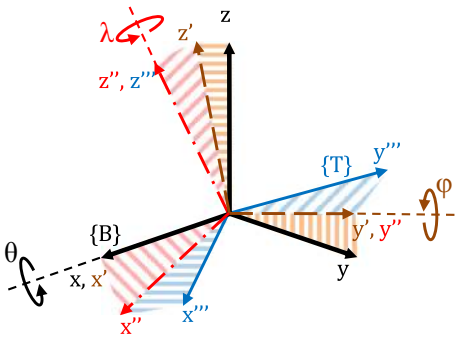

Fig. 12 Rotation from moving frame {T} to fixed coordinate frame {B} using Euler angles θ, φ and λ

$$\boldsymbol{\omega}_{\mathrm{MP}} = \begin{bmatrix} 1 & 0 & \mathrm{s}\,\varphi \\ 0 & \mathrm{c}\theta & -\mathrm{s}\theta\mathrm{c}\,\varphi \\ 0 & \mathrm{s}\theta & \mathrm{c}\theta\mathrm{c}\,\varphi \end{bmatrix} \begin{Bmatrix} \dot{\theta} \\ \dot{\varphi} \\ \dot{\lambda} \end{Bmatrix} = \mathbf{U} \begin{Bmatrix} \dot{\theta} \\ \dot{\varphi} \\ \dot{\lambda} \end{Bmatrix} \tag{108}$$

Furthermore, by time differentiating of Eqs. (107) or (108), the angular acceleration of the MP can be obtained as below

$$\begin{aligned} \dot{\boldsymbol{\omega}}_{\mathrm{MP}} &= \ddot{\theta}\hat{\mathbf{i}} + \ddot{\varphi}\hat{\mathbf{j}}' + \dot{\varphi}\left(\dot{\theta}\hat{\mathbf{i}} \times \hat{\mathbf{j}}'\right) \\ &\quad + \ddot{\lambda}\hat{\mathbf{k}}'' + \dot{\lambda}\left\{\left(\dot{\theta}\hat{\mathbf{i}} + \dot{\varphi}\hat{\mathbf{j}}'\right) \times \hat{\mathbf{k}}''\right\} \\ &= \mathbf{U}\begin{Bmatrix} \ddot{\theta} \\ \ddot{\varphi} \\ \ddot{\lambda} \end{Bmatrix} + \dot{\mathbf{U}}\begin{Bmatrix} \dot{\theta} \\ \dot{\varphi} \\ \dot{\lambda} \end{Bmatrix} \end{aligned} \tag{109}$$

where

$$\dot{\mathbf{U}} = \begin{bmatrix} 0 & 0 & \dot{\varphi}\mathrm{c}\varphi \\ 0 & -\dot{\theta}\mathrm{s}\theta & -\dot{\theta}\mathrm{c}\theta\mathrm{c}\varphi + \dot{\varphi}\mathrm{s}\theta\mathrm{s}\varphi \\ 0 & \dot{\theta}\mathrm{c}\theta & -\dot{\theta}\mathrm{s}\theta\mathrm{c}\varphi - \dot{\varphi}\mathrm{c}\theta\mathrm{s}\varphi \end{bmatrix} \tag{110}$$

References

1. Kamali, K., Akbarzadeh, A.: A novel method for direct kinematics solution of fully parallel manipulators using basic regions theory. J. Syst. Control Eng. **225**(5), 683–701 (2011)
2. Akbarzadeh, A., Enferadi, J.: A virtual work based algorithm for solving direct dynamics problem of a 3-RRP spherical parallel manipulator. J. Intell. Robot. Syst. **63**, 25–49 (2011)
3. Akbarzadeh, A., Enferadi, J., Sharifnia, M.: Dynamics analysis of a 3-RRP spherical parallel manipulator using the natural orthogonal complement. Multibody Syst. Dyn. **29**(4), 361–380 (2013)
4. Kordjazi, H., Akbarzadeh, A.: Inverse dynamics of a 3-prismatic–revolute–revolute planar parallel manipulator using natural orthogonal complement. Proc. Inst. Mech. Eng. Part I J. Syst. Control Eng. **225**(3), 258–269 (2011)
5. Pedrammehr, S., Mahboubkhah, M., Khani, N.: Improved dynamic equations for the generally configured Stewart platform manipulator. J. Mech. Sci. Technol. **26**(3), 711–721 (2012)
6. Do, W.Q.D., Yang, D.C.H.: Inverse dynamic analysis and simulation of a platform type of robot. J. Robot. Syst. **5**(3), 209–227 (1998)
7. Dasgupta, B., Mruthyunjaya, T.S.: A Newton–Euler formulation for the inverse dynamics of Stewart platform manipulator. Mech. Mach. Theory **33**(8), 1135–1152 (1998)
8. Dasgupta, B., Mruthyunjaya, T.S.: Closed-form dynamic equations of the general Stewart platform through Newton–Euler approach. Mech. Mach. Theory **33**(7), 993–1012 (1998)
9. Fu, S., Yao, Y., Wu, Y.: Comments on "A Newton–Euler formulation for the inverse dynamics of the Stewart platform manipulator". Mech. Mach. Theory **42**, 1668–1671 (2007)
10. Geng, Z., Haynes, L.S., Lee, J.D., Carroll, R.L.: On the dynamic model and kinematic analysis of a class of Stewart platforms. Robot. Auton. Syst. **9**(4), 237–254 (1992)
11. Lebret, G., Liu, K., Lewis, F.L.: Dynamic analysis and control of a Stewart platform manipulator. J. Robot. Syst. **10**(5), 629–655 (1993)
12. Ting, Y., Chen, Y.S., Jar, H.C.: Modeling and control for a Gough–Stewart platform CNC machine. J. Robot. Syst. **21**(11), 609–623 (2004)
13. Wang, W., Yang, H.Y., Zou, J., Ruan, X.D., Fu, X.: Optimal design of Stewart platforms based on expanding the control bandwidth while considering the hydraulic system design. J. Zhejiang Univ. Sci. A **10**(1), 22–30 (2009)
14. Guo, H.B., Li, H.R.: Dynamic analysis and simulation of a six degree of freedom Stewart platform manipulator. Proc. Inst. Mech. Eng. Part C J. Mech. Eng. Sci. **220**, 61–72 (2006)
15. Tsai, L.W.: Solving the inverse dynamics of Stewart–Gough manipulator by the principle of virtual work. J. Mech. Des. **122**, 3–9 (2000)
16. Abedinnasab, M.H., Vossoughi, G.R.: Analysis of a 6-DOF redundantly actuated 4-legged parallel mechanism. Nonlinear Dyn. **58**(1–2), 611–622 (2009)
17. Liu, M.J., Li, C.X., Li, C.N.: Dynamics analysis of the Gough–Stewart platform manipulator. IEEE Trans. Robot. Autom. **16**(1), 94–98 (2000)
18. Khalil, W., Guegan, S.: Inverse and direct dynamic modeling of Gough–Stewart robots. IEEE Trans. Robot. Autom. **20**(4), 754–762 (2004)
19. Huang, X., Liao, Q., Wei, Sh: Closed-form forward kinematics for a symmetrical 6–6 Stewart platform using algebraic elimination. Mech. Mach. Theory **45**(2), 327–334 (2010)
20. Lee, T.Y., Shim, J.K.: Forward kinematics of the general 6–6 Stewart platform using algebraic elimination. Mech. Mach. Theory **36**(9), 1073–1085 (2001)
21. Husty, M.L.: An algorithm for solving the direct kinematics of general Stewart–Gough platforms. Mech. Mach. Theory **31**(4), 365–379 (1996)
22. Rolland, L.: Synthesis of the forward kinematics problem algebraic modeling for the general parallel manipulator: displacement-based equations. Adv. Robot. **21**(9), 1071–1092 (2007)
23. Rolland, L.: Certified solving of the forward kinematics problem with an exact algebraic method for the general parallel manipulator. Adv. Robot. **19**(9), 995–1025 (2005)

24. Nanua, P., Waldron, K.J., Murthy, V.: Direct kinematic solution of a Stewart platform. IEEE Trans. Robot. Autom. **6**(4), 438–443 (1990)
25. Innocenti, C., Parenti-Castelli, V.: Direct position analysis of the Stewart platform mechanism. Mech. Mach. Theory **25**(6), 611–621 (1990)
26. Dasgupta, B., Mruthyunjay, T.S.: The Stewart platform manipulator: a review. Mech. Mach. Theory **35**, 15–40 (2000)
27. Innocenti, C.: Forward kinematics in polynomial form of the general Stewart platform. Trans. ASME J. Mech. Des. **123**, 254–260 (2001)
28. Ku, D.M.: Direct displacement analysis of a Stewart platform mechanism. Mech. Mach. Theory **34**, 453–465 (1999)
29. Liu, K., Fitzgerzld, J.M., Lewis, F.L.: Kinematic analysis of a Stewart platform manipulator. IEEE Trans. Ind. Electron. **40**(2), 282–293 (1993)
30. Parikh, P., Lam, S.: A hybrid strategy to solve the forward kinematics problem in parallel manipulators. IEEE Trans. Robot. **21**(1), 18–25 (2005)
31. Darvishi, M.T., Barati, A.: A third-order Newton-type method to solve systems of nonlinear equations. Appl. Math. Comput. **187**(2), 630–635 (2007)
32. Kardan, I., Akbarzadeh, A.: An improved hybrid method for forward kinematics analysis of parallel robots. Adv. Robot. **29**(6), 401–411 (2015)
33. McPhee, J., Shi, P., Piedbuf, J.C.: Dynamics of multibody systems using virtual work and symbolic programming. Math. Comput. Modell. Dyn. Syst. Methods Tools Appl. Eng. Relat. Sci. **8**(2), 137–155 (2002)
34. Gallardo, J., Rico, J.M., Frisoli, A., Checcacci, D., Bergamasco, M.: Dynamics of parallel manipulators by means of screw theory. Mech. Mach. Theory **38**, 1113–1131 (2003)
35. Xi, F., Sinatra, R.: Inverse dynamics of hexapods using the natural orthogonal complement method. J. Manuf. Syst. **21**(2), 73–82 (2002)